AD NUMBER: AD0882195

LIMITATION CHANGES

TO:

Approved for public release; distribution is unlimited.

FROM:

Distribution authorized to US Government Agencies and their Contractors; Export Control; 26 Feb 1971. Other requests shall be referred to Naval Ordnance Lab, Silver Spring, MD, 20910.

AUTHORITY

Per USNSWC ltr dtd 4 Dec 1974

NOLTR 71-29

EFFECT OF FINITE SAMPLING RATES ON SMOOTHING THE OUTPUT OF A SQUARE LAW DETECTOR WITH NARROW BAND INPUT

By
C. Nicholas Pryor

26 FEBRUARY 1971

NOL
NAVAL ORDNANCE LABORATORY, WHITE OAK, SILVER SPRING, MARYLAND 20910

NOLTR 71-29

NOLTR 71-29

EFFECT OF FINITE SAMPLING RATES ON SMOOTHING THE OUTPUT OF A SQUARE LAW DETECTOR WITH NARROW BAND INPUT

by:

C. Nicholas Pryor

ABSTRACT: Most modern spectral analysis systems time-share a single narrow-band filter and detector among a large number of frequency channels and thus provide sampled rather than continuous data to output averaging devices. For practical filter designs and finite sampling rates, a loss in performance is experienced due to this sampling. Analytical means are developed for computing this loss, and the loss is evaluated for a number of common filter shapes. Losses of 1 to 2 dB are shown to occur when the detector is sampled at rates comparable to the detector bandwidth.

Physics Research Department
NAVAL ORDNANCE LABORATORY
WHITE OAK, MARYLAND

NOLTR 71-29 26 February 1971

EFFECT OF FINITE SAMPLING RATES ON SMOOTHING THE OUTPUT OF A SQUARE LAW DETECTOR WITH NARROW BAND INPUT

This report develops an analytical method for calculating one loss due to sampling in spectral analysis systems and contains examples for a number of commonly used filter functions. The results should be of interest to those engaged in designing or evaluating systems employing spectral analysis or other narrow band filtering operations. The work was performed in the Electronics and Electromagnetics Division of the Physics Research Department and was funded by the Naval Air Systems Command under AIRTASK A370-370A-WF08-121-703, Signal Processing.

GEORGE G. BALL
Captain, USN
Commander

Z. I. SLAWSKY
By direction

CONTENTS

ILLUSTRATIONS

SUMMARY OF NOTATION

B	Nominal bandwidth of narrow-band analysis filter; not necessarily related to 3 dB bandwidth or noise bandwidth.
E	Efficiency of sampling process between detector output and averager input, defined as F_e/F_o.
E_n	Sampling efficiency for the noise-induced component of the square-law detector output, defined as F_{e_n}/F_n.
E_s	Sampling efficiency for the signal-induced component of the square-law detector output, defined as F_{e_s}/F_s.
F	Sampling frequency used in sampler between detector output and averager input.
F_c	Center frequency of narrow-band analysis filter.
F_e	Effective rate of independent samples into averager, defined as $\sigma_i^2/\sigma_o^2 T$.
F_n	Limit of F_e for noise-induced variance component at square-law detector output, as F approaches infinity.
F_o	Limit of F_e as sampling frequency F approaches infinity.
F_s	Limit of F_e for signal-induced variance component at square-law detector output, as F approaches infinity.
$H(\omega)$	Amplitude transfer function of narrow-band analysis filter.
N	Noise power spectral density (watts/Hz for single-sided spectrum) at input to narrow-band analysis filter.
NBW	Noise Bandwidth of narrow-band analysis filter, defined as P/N.
P	Noise power output of narrow-band analysis filter.
$\phi_{nn}(\tau)$	Autocorrelation function of noise-induced variance component at output of square-law detector.
$_n\phi_{nn}(\tau)$	Normalized autocorrelation of noise-induced variance component, defined as $\phi_{nn}(\tau)/\phi_{nn}(0)$.

$\phi_{ss}(\tau)$ Autocorrelation function of signal-induced variance component at output of square-law detector.

$_{n}\phi_{ss}(\tau)$ Normalized autocorrelation of signal-induced variance component, defined as $\phi_{ss}(\tau)/\phi_{ss}(0)$.

$\phi_{xx}(\tau)$ Autocorrelation function of input fluctuations to sampler.

$_{n}\phi_{xx}(\tau)$ Normalized autocorrelation function of sampler input fluctuations, defined as $\phi_{xx}(\tau)/\phi_{xx}(0)$.

$\Phi_{nn}(\omega)$ Double-sided power density spectrum of noise-induced variance component at output of square-law detector, Fourier transform of $\phi_{nn}(\tau)$.

$_{n}\Phi_{nn}(\omega)$ Normalized double-sided density spectrum of noise-induced variance component, Fourier transform of $_{n}\phi_{nn}(\tau)$.

$\Phi_{ss}(\omega)$ Double-sided power density spectrum of signal-induced variance component at output of square-law detector, Fourier transform of $\phi_{ss}(\tau)$.

$_{n}\Phi_{ss}(\omega)$ Normalized double-sided power density spectrum of signal-induced variance component, Fourier transform of $_{n}\phi_{ss}(\tau)$.

$\Phi_{xx}(\omega)$ Double-sided power density spectrum of input to sampler, Fourier transform of $\phi_{xx}(\tau)$.

$_{n}\Phi_{xx}(\omega)$ Normalized double-sided power density spectrum of sampler input, Fourier transform of $_{n}\phi_{xx}(\tau)$.

σ_i^2 Variance of sampler or averager input.

σ_o^2 Variance of averager output.

T Uniform integration time used in averager.

BLANK PAGE

INTRODUCTION

Modern spectral analysis systems often take the form shown in Fig. 1 where the input is passed through a narrow band filter and detected, and the detector output is then passed through a low-pass filter (or averager) for further smoothing. Most systems do not use the purely parallel analog approach shown in Fig. 1, but instead simulate it by sharing a single spectrum analyzer filter and detector over many channels and forming periodic estimates of the input to the averaging filter. Both swept-filter time-compression systems and digital Fast Fourier Transform processors fall into this category. The result is equivalent to sampling the detector output at some rate generally near the bandwidth of the analysis filter. For time compression processors the sampling rate is equal to the number of sweeps per second, while for FFT processors the sampling rate equals the number of transforms computed per second.

While sampling at a rate equal to the filter bandwidth can be shown to be an information lossless operation when the analysis filter has infinitely steep skirts, some loss is generally incurred in the sampling process in practical systems. This report develops the procedure for evaluating this loss and shows the results for a number of commonly used filter functions. The detector following the narrow-band filter is assumed in this report to be a square-law detector, primarily for mathematical convenience. Spectral analysis systems often substitute other detectors, such as full wave or envelope detectors, for the square-law detector to reduce the required dynamic range. While the results obtained here are not strictly applicable to such systems, they may still be used to a first approximation to estimate the effects of sampling in those systems.

THEORY

The averaging filter with its sampled input can be represented as a system which averages discrete inputs over some period of time T. If the input samples are uncorrelated, this averaging system reduces the variance of its input by a factor equal to the number of independent samples received in the time T. If the samples are correlated, the variance is reduced by a smaller amount. However, this reduction can still be described by an effective sampling rate F_e such that (as the definition of F_e)

$$\frac{\sigma_o^2}{\sigma_i^2} = \frac{1}{F_e T} \qquad (1)$$

for the averaging filter. The effective sampling rate depends on the actual sampling rate at the averager input and on the shape of the analyzer bandpass filter function. The problem in determining the effectiveness of the averaging filter is then reduced to one of determining the effective sampling rate F_e at its input.

Appendix A, which originally appeared as an internal Naval Ordnance Laboratory report, provides a means of computing F_e for such averaging systems if the input spectrum or autocorrelation function to the sampler is known. This result is given as

$$F_e = \frac{F}{\sum_{k=-\infty}^{\infty} {}_n\phi_{xx}(k/F)} \tag{2a}$$

$$= \frac{1}{\sum_{n=-\infty}^{\infty} {}_n\phi_{xx}(2\pi nF)} \tag{2b}$$

where F is the actual sampling frequency and ${}_n\phi_{xx}(\tau)$ and ${}_n\phi_{xx}(\omega)$ are respectively the autocorrelation function and the ${}_n\phi_{xx}$ double-sided power density spectrum of the input to the sampler, both normalized for unity total power. A limiting value F_o for the effective sampling rate is also obtained in the form

$$F_o = \frac{1}{\int_{-\infty}^{\infty} {}_n\phi_{xx}(\tau)\, d\tau} \tag{3a}$$

$$= \frac{1}{{}_n\phi_{xx}(0)} \tag{3b}$$

when the actual sampling rate is raised to infinity or when continuous signals are used. The ratio F_e/F_o of these quantities may be considered to be the efficiency E of the sampling process, in the sense that it represents the fraction of the total number of independent samples (or degrees of freedom) surviving the sample process. The output variance of the averager will be increased by the factor $1/E$ due to the sampling process, relative to a system without sampling at the detector output. Thus the equations

$$E = \frac{F\int_{-\infty}^{\infty}\phi_{xx}(\tau)\,d\tau}{\sum_{k=-\infty}^{\infty}\phi_{xx}(k/F)} \qquad (4a)$$

$$= \frac{\phi_{xx}(0)}{\sum_{k=-\infty}^{\infty}\phi_{xx}(2\pi nF)} \qquad (4b)$$

may be used to compute the sampling efficiency, using either the autocorrelation function or the power density spectrum of the detector output. The requirement for using normalized values of the functions is removed because normalization does not affect the ratio of F_e and F_o. These results as derived in Appendix A assume that the averaging time T is appreciably larger than the inverse of the analysis filter bandwidth which is equivalent to saying that substantial reduction of the variance is desired from the post-detection averaging. This assumption is met in all practical cases where post-detection averaging is used.

Appendix B provides a means of computing the low-pass noise spectrum $\phi_{xx}(\omega)$ at the square law detector output for a given signal and noise power input when the shape of the analysis filter is known. The input to the square law detector is assumed to be a sinusoidal signal of power S plus a narrow-band noise of power P centered around the signal frequency. The detector output consists of a steady-state component of mean value P+S (which equals the input power to the detector) plus random fluctuations with autocorrelation function of the form

$$\phi_{xx}(\tau) = P^2{}_n\phi_{nn}(\tau) + 2PS_n\phi_{ss}(\tau) \qquad (5)$$

Each of the autocorrelation functions ${}_n\phi_{nn}(\tau)$ and ${}_n\phi_{ss}(\tau)$ is normalized to unity at $\tau = 0$ so the coefficients represent the contribution each makes to the variance $\sigma_i^2 = \phi_{xx}(0)$ at the detector output. Notice that the first term produces a variance P^2 and appears whether signal is present at the detector input or not. This will be referred to in this report as the "noise-induced" component of the detector variance since it depends on P alone. The second term produces a variance 2PS and is present only when a signal appears in addition to the noise at the detector input, and thus will be termed the "signal-induced" component of the variance.

The noise-induced term is actually the more interesting of the two in most system performance calculations since the false alarm rate of a detection system is determined with the signal component equal to zero. Thus only the characteristics of the noise-induced term are required for determining false alarm parameters.

As shown in Appendix B, the spectrum ${}_n\phi_{ss}(\omega)$ of the signal-induced component is identical in form to the power transfer function $|H(\omega)|^2$ of the narrow-band filter when translated down to a zero center frequency. The spectrum ${}_n\phi_{nn}(\omega)$ of the noise-induced component is obtained from ${}_n\phi_{ss}(\omega)$ as the autoconvolution

$$ {}_n\phi_{nn}(\omega) = (1/2\pi) \int_{-\infty}^{\infty} {}_n\phi_{ss}(\omega) \; {}_n\phi_{ss}(\alpha-\omega) \; d\alpha \qquad (6a) $$

or in the time domain

$$ {}_n\phi_{nn}(\tau) = {}_n\phi_{ss}{}^2(\tau) \qquad (6b) $$

While it is possible to determine the complete spectrum $\phi_{xx}(\omega)$ of the detector output for a given filter shape and given values of P and S and calculate the averager performance from this, it is more convenient to separate the two components and treat them individually. A procedure for calculating the mean and variance σ_o^2 at the output of the averager then consists of the following steps:

(1) From the bandwidth and shape function of the narrow-band analysis filter, determine the noise bandwidth NBW of the filter as

$$ NBW = (1/2\pi) \int_{0}^{\infty} |H(\omega)|^2 \, d\omega \qquad (7) $$

This result happens to be identical to the limiting sampling rate F_s for the signal-induced variance component which is used later.

(2) Multiply the one-sided power spectral density N of the noise input to the analyzer by the noise bandwidth to obtain the filter noise output P. The mean value P+S of the averager output may now be determined as well as the contributions of each of the two variance components at the detector output.

(3) By translating $|H(\omega)|^2$ down to zero center frequency to determine $\phi_{ss}(\omega)$ and using equations (3) and (4), determine the limiting effective sampling rate F_s and the sampling efficiency E_s for finite sampling rates for the signal-induced component of the variance.

(4) Obtain $\phi_{nn}(\omega)$ or the corresponding autocorrelation function and use equations (3) and (4) again to obtain the limiting effective sampling rate F_n and the sampling efficiency E_n for the noise-induced component.

(5) Determine the output variance from the averager in the absence of sampling as

$$\sigma_o^2 = (P^2/F_n + 2PS/F_s)/T \qquad \text{(unsampled)}$$

and the output variance for the sampled case as

$$\sigma_o^2 = (P^2/E_nF_n + 2PS/E_sF_s)/T \qquad \text{(sampled)}$$

The remaining sections of this report treat commonly used filter functions to obtain the parameters necessary to perform the above steps. Table 1 lists the 3 dB bandwidth, the noise bandwidth, and the limiting rates F_s and F_n for each filter shape, and Fig. 2 shows the bandpass function for each. The functions E_s and E_n are plotted versus sampling frequency for each filter type in Figs. 3 through 8.

IDEAL BANDPASS FILTER

The idealized form of the bandpass filter in a spectrum analyzer is one with a flat response over a frequency band B and zero response outside this band, or

$$H(\omega) = \begin{cases} 1 & F_c - B/2 < |\omega/2\pi| < F_c + B/2 \\ 0 & \text{elsewhere} \end{cases}$$

This response function is shown in Fig. 2a. F_c is the center frequency of the filter and is assumed to be large compared to B here and for all other filter forms. The noise bandwidth is the integral of $|H^2(\omega)|$ over positive frequencies and is obviously equal to B. The spectrum of the signal-induced fluctuations from the detector is found by translating $|H^2(\omega)|$ down to baseband and normalizing for unity total area and thus is

$${}_n\Phi_{ss}(\omega) = \begin{cases} 1/B & |\omega/2| < B/2 \\ 0 & \text{elsewhere} \end{cases}$$

while the spectrum of the noise-induced component is obtained from the autoconvolution of ${}_n\Phi_{ss}(\omega)$ and is

$${}_n\Phi_{nn}(\omega) = \begin{cases} (1/B)(1 - |\omega|/2\pi B) & |\omega/2\pi| < B \\ 0 & \text{elsewhere} \end{cases}$$

For each of these two components the limiting effective sampling rate (F_s or F_n) is also equal to B. However, the efficiencies (E_s and E_n) for finite sampling rates as obtained from equation (4b) are different for the two components.

For the signal-induced component, the term

$$\sum_{n=-\infty}^{\infty} {}_n\Phi_{ss}(2\omega nF)$$

has only one non-zero component, equal to 1/B for sampling frequencies F above B/2. The sampling efficiency is thus unity for these sampling frequencies. For values of F between B/4 and B/2, the summation contains three terms of value 1/B and the sampling efficiency drops to 1/3 in this range. Similarly, the efficiency E is equal to 1/5 if the sampling frequency lies between B/6 and B/4, and the efficiency continues to drop in this stairstep fashion for lower values of F as shown by the dashed curve in Figure 3. For low sampling frequencies the efficiency is very nearly equal to F/F_s, since the individual samples become nearly independent.

For the noise-induced component, ${}_n\Phi_{nn}(\omega)$ must be substituted into equation (4b). Since ${}_n\Phi_{nn}(\omega)$ is zero above the frequency B, the sampling efficiency is again unity for sampling frequencies in excess of B. For values of F between B/2 and B, three terms appear in the summation and can be evaluated as

$$E_n = \frac{1}{1+2(1-F/B)} = \frac{1}{3-2F/B} \qquad B/2 < F < B$$

and reaches the value 1/2 when F equals B/2. When F lies in the range between B/3 and B/2 the summation has five non-zero terms and can be written

$$E_n = \frac{1}{1+2(1-F/B)+2(1-2F/B)} = \frac{1}{5-6F/B} \qquad B/3 < F < B/2$$

This argument can be continued for progressively lower frequencies.

The sampling efficiency for the noise-induced component is also shown in Fig. 3. Notice that in this case it never exceeds the slope F/F_n and that it converges to F/F_n very rapidly for sampling frequencies below B. The different behavior of the sampling efficiency for the two components is rather interesting. For sampling frequencies above B, both components have unity sampling efficiency and nothing is lost in the sampling process. However, for a sampling frequency just slightly above B/2, the efficiency is still unity for the signal-induced variance while only half as much smoothing takes place on the more critical noise-induced component of the variance.

At a slightly lower sampling frequency just below B/2 the sampling efficiency on the signal-induced term drops suddenly to 1/3 while no significant change occurs in the efficiency for the noise-induced term. This discontinuity in the behavior is, of course, due to the infinite slopes on the sides of the ideal filter response curve.

SINGLE-TUNED RESONANT FILTER

The simplest form of analog filter for use in a spectrum analyzer consists of a single pole pair in its transfer function. This type of circuit has a power response

$$|H(\omega)|^2 = \frac{(B/2)^2}{(B/2)^2+(\omega/2\pi-F_c)^2}$$

where F_c is the center frequency and B is the bandwidth between the 3 dB (half-power) points on the response, as shown in Fig. 2b. Translated down to zero frequency this gives a low-pass spectrum

$$\phi_{ss}(\omega) = \frac{1}{1+(\omega/\pi B)^2} \qquad \text{(unnormalized)}$$

Taking the Fourier transform of this function yields the autocorrelation function $\phi_{ss}(\omega)$ as

$$\phi_{ss}(\tau) = (\pi B/2)\exp(-\pi B\,|\tau|)$$

The factor $\pi B/2$ in the unnormalized autocorrelation is the total area under $\phi_{ss}(\omega)$ and thus represents the noise bandwidth and F_s for the signal-induced variance out of the square law detector.

The spectrum of the noise-induced variance is found by normalizing and squaring $\phi_{ss}(\tau)$ and transforming back to the frequency domain. This gives

$${}_n\phi_{nn}(\omega) = (1/\pi B)\,\frac{1}{1+(\omega/2\pi B)^2}$$

The limiting effective sampling rate F_n for the noise-induced component is $1/{}_n\phi_{nn}(0)$ or πB. Note that this limiting sampling rate is twice that obtained for the signal-induced component so that the noise-induced term has twice as much effective smoothing as the signal-induced term if the sampling rate is sufficiently high.

The efficiency E_s for smoothing the signal-induced component as a function of the sampling frequency F may be found from equation (4a) as

$$E_s = \frac{F}{(\pi B/2)\sum_{k=-\infty}^{\infty} \exp|-\pi Bk/F|} = \frac{(2F/\pi B)}{1+2\sum_{k=1}^{\infty} \exp(-\pi Bk/F)}$$

$$= \frac{(2F/\pi B)}{1+2\exp(-\pi B/F)/[1-\exp(-\pi B/F)]}$$

$$= (2F/\pi B)\,\frac{1-\exp(-\pi B/F)}{1+\exp(-\pi B/F)}$$

This function is plotted in Fig. 4 as a function of sampling frequency F. Note that for small F the exponential term vanishes and the efficiency is simply $2F/\pi B$ or F/F_s. For large F the efficiency assymptotically approaches unity and is equal to about 59% when the detector output is sampled at the nominal bandwidth B. Sampling at about 2.7B is required to reach a sampling efficiency of 90%.

The noise-induced term of the detector variance has the same spectral shape as the signal-induced term, but twice the bandwidth. Thus its sampling efficiency may be written directly as

$$E_n = (F/\pi B)\,\frac{1-\exp(-2\pi B/F)}{1+\exp(-2\pi B/F)}$$

and also is plotted in Fig. 4. Note this function also follows F/F_n for low sampling frequencies (where the F_n for this term is πB) and that it has only reached 32% for sampling at a rate equal to the nominal filter bandwidth B. The sampling efficiency for this term is only 75% when sampling at three times the nominal bandwidth and a sampling rate of nearly 6B would be required to reach 90% efficiency. Thus some of the additional smoothing available on the noise-induced term relative to that on the signal-induced term is lost when sampling is done at a finite rate.

THIRD-ORDER BUTTERWORTH FILTER

Multipole analog filters are often used to sharpen the response of the spectrum analyzer bandpass filter relative to that of the single resonant circuit. This is done primarily to reduce response of a narrow-band channel to strong signals in nearby frequency bins. A typical choice is a three pole pair circuit giving 18 dB per octave skirts on the response. The Butterworth design gives maximally flat ripple-free response in the passband and has a power response given by

$$|H(\omega)|^2 = \frac{(B/2)^6}{(B/2)^6+(\omega/2\pi-F_c)^6}$$

where F_c is again the center frequency and B is the bandwidth between the 3 dB points in the response. This response curve is shown in Fig. 2c. The corresponding $\phi_{ss}(\omega)$ as a low-pass spectrum is

$$\phi_{ss}(\omega) = \frac{1}{1+(\omega/\pi B)^6} \qquad \text{(unnormalized)}$$

The autocorrelation function $\phi_{ss}(\tau)$ can be obtained by taking a partial fraction expansion of $\Phi_{ss}(\omega)$ and transforming each term to give a complex form

$$\phi_{ss}(\tau) = (\pi B/12)[2\exp(-\pi B|\tau|) + (1+j\sqrt{3})\exp(-1-j\sqrt{3})(\pi B|\tau|/2)$$

$$+ (1-j\sqrt{3})\exp(-1+j\sqrt{3})(\pi B|\tau|/2)] \qquad \text{(unnormalized)}$$

The value of $\phi_{ss}(0)$ is $\pi B/3$ and this is the noise bandwidth of the Butterworth filter as well as the value of F_s for the signal-induced variance term.

The sampling efficiency E_s is obtained from equation (4a) using the fact that

$$\sum_{k=-\infty}^{\infty} \exp(a|k|/F) = \frac{1+\exp(a/F)}{1-\exp(a/F)}$$

whenever the real part of a is negative. The denominator of equation (4a) can thus be written as

$$\sum_{k=-\infty}^{\infty} \phi_{ss}(k/F) = (\pi B/12)\left\{ 2\left[\frac{1+\exp(-\pi B/F)}{1-\exp(-\pi B/F)}\right]\right.$$

$$+ (1+j\sqrt{3})\left[\frac{1+\exp(-1-j\sqrt{3})(\pi B/2F)}{1-\exp(-1-j\sqrt{3})(\pi B/2F)}\right]$$

$$\left. + (1-j\sqrt{3})\left[\frac{1+\exp(-1+j\sqrt{3})(\pi B/2F)}{1-\exp(-1+j\sqrt{3})(\pi B/2F)}\right]\right\}$$

$$= (\pi B/6)\left\{\left[\frac{1+\exp(-\pi B/F)}{1-\exp(-\pi B/F)}\right]\right.$$

$$\left. + \frac{[1-\exp(-\pi B/F)] + 2\sqrt{3}\exp(-\pi B/2F)\sin(\sqrt{3}\pi B/2F)}{[1+\exp(-\pi B/F)] - 2\exp(-\pi B/2F)\cos(\sqrt{3}\pi B/2F)}\right\}$$

Dividing F by this function, as prescribed by equation (4a), then gives the sampling efficiency as shown in Fig. 5. The limiting value of E_s for high sampling frequencies is, of course, unity, and the asymptotic behavior for low F is approximately $3F/\pi B$ or F/F_s. Note that the sampling efficiency exceeds the asymptotic value over the range of sampling frequencies between about B/2 and B. This behavior is similar to that seen in the ideal filter case and presumably is due to the steep filter skirts.

The autocorrelation function of the noise-induced variance component may be obtained by normalizing and squaring $\phi_{ss}(\tau)$ to give

$$n\phi_{nn}(\tau) = (1/16)\ [2\exp(-\pi B|\tau|)$$

$$+ (1+j\sqrt{3})\exp(-1-j\sqrt{3})(\pi B|\tau|/2)$$

$$+ (1-j\sqrt{3})\exp(-1+j\sqrt{3})(\pi B|\tau|/2)]^2$$

$$= (1/8)\ [2\exp(-2\pi B|\tau|) + 4\exp(-\pi B|\tau|)$$

$$+ (-1+j\sqrt{3})\exp(-1-j\sqrt{3})\pi B|\tau| + (-1-j\sqrt{3})\exp(-1+j\sqrt{3})\pi B|\tau|$$

$$+ 2(1+j\sqrt{3})\exp(-3-j\sqrt{3})\pi B|\tau|/2 + 2(1-j\sqrt{3})\exp(-3+j\sqrt{3})$$

$$\pi B|\tau|/2]$$

Using the integral

$$\int_{-\infty}^{\infty} \exp(a|\tau|)\, d\tau = -2/a$$

for all a with negative real part, the integral of ${}_n\phi_{nn}(\tau)$ may be found from its six exponential components and used in equation (3a) to determine F_n for the noise-induced variance component as $2\pi B/5$.

The sampling efficiency E_n is found from equation (4a) where the numerator is $5F/2\pi B$ and the denominator is found by evaluating the indicated summation over each of the exponential terms to give

$$\sum_{k=-\infty}^{\infty} {}_n\phi_{nn}(k/F) = (1/4)\left[\frac{1+\exp(-2\pi B/F)}{1-\exp(-2\pi B/F)} + 2\,\frac{1+\exp(-\pi B/F)}{1-\exp(-\pi B/F)} \right.$$

$$- \frac{1-\exp(-2\pi B/F) - 2\sqrt{3}\,\exp(-\pi B/F)\sin\sqrt{3}\,\pi B/F}{1+\exp(-2\pi B/F) - 2\exp(-\pi B/F)\cos\sqrt{3}\,\pi B/F}$$

$$\left. +2\,\frac{1-\exp(-3\pi B/F) + 2\sqrt{3}\,\exp(-3\pi B/2F)\sin\sqrt{3}\,\pi B/2F}{1+\exp(-3\pi B/F) - 2\exp(-3\pi B/2F)\cos\sqrt{3}\,\pi B/2F} \right]$$

The resultant sampling efficiency as a function of sampling frequency F is shown in Fig. 5. Again, the efficiency goes as $5F/2\pi B$ or F/F_n for low sampling frequencies and approaches unity for high sampling rates. Since the much sharper cutoff on the skirts of the 3 pole pair filter reduces the high frequency information at the detector output relative to that produced by the single pole pair of the single-tuned resonant filter, the sampling efficiency approaches unity much more rapidly. Sampling the averager input at the nominal filter bandwidth B gives a sampling efficiency of 97% for the signal-induced component and 80% for the noise-induced component. The sampling efficiency is essentially unity for both components if the sampling frequency is 2B or higher.

The results shown in Fig. 5 were obtained specifically for the Butterworth type filter. However, quite similar results could be expected for other designs such as Popoulis or low-ripple Tchebycheff filters with the same number of poles. As the number of pole pairs increases above three, the values of F_s and F_n become closer to B and the efficiencies E_s and E_n more nearly resemble those for the ideal filter.

GAUSSIAN FILTER

Bandpass filters are sometimes built as multipole approximations to the Gaussian function because of the desirable physical, as well as analytical, properties of this function. The power response of the Gaussian filter may be described as

$$|H(\omega)|^2 = \exp\left[-\ (\omega/2\pi - F_c)^2\ /B^2\right]$$

where F_c again is the center frequency and B is the frequency deviation to the point of inflection (one "standard deviation") on the amplitude response curve. This response function is shown in Fig. 2d. Note that B as defined here is not the "3 dB bandwidth" since the response is down only about 1.1 dB at points plus or minus B/2 from the center frequency. The bandwidth between the 3 dB points is about 1.67 B.

The low-pass form of the response function defines $\Phi_{ss}(\omega)$ and is

$$\Phi_{ss}(\omega) = \exp\left[-\ (\omega/2\pi B)^2\right] \qquad \text{(unnormalized)}$$

Integrating over this spectrum gives the noise bandwidth and the limiting sampling rate F_s for the signal-induced component as $\sqrt{\pi}$ B. The spectrum $\Phi_{nn}(\omega)$ of the noise-induced component is the autoconvolution of $\Phi_{ss}(\omega)$ and is

$$\Phi_{nn}(\omega) = K \exp\left[-\ (\omega/2\pi B)^2/2\right]$$

where K is an unimportant constant. This spectrum is of the same form as $\Phi_{ss}(\omega)$ except that the bandwidth is effectively larger by a factor of $\sqrt{2}$. Thus the limiting effective sampling rate F_n for the noise-induced component of the detector variance is $\sqrt{2\pi}$ B.

A closed form expression for E_s and E_n cannot be obtained for the Gaussian filter, but convergence of the series is rapid enough to allow numerical evaluation of equation (4b). The results are shown in Fig. 6. While the sampling efficiencies are rather low for sampling at a frequency equal to the nominal bandwidth B, this is primarily due to the way in which the filter bandwidth was defined. Sampling at a frequency equal to the "3 dB bandwidth" of 1.67 B gives sampling efficiencies of 89% and 66% respectively for the signal-induced and noise induced variance components, while sampling at a 50% higher rate (2.5 B) gives sampling efficiencies of 99% and 92% respectively. Convergence to the limiting sampling rate is thus fairly rapid.

UNWEIGHTED CORRELATOR

Digital spectrum analyzers generally operate either by repeatedly performing a Fourier transform on a fixed length sample of input signal or by crosscorrelating the input signal with stored replicas of sine waves. Either approach corresponds to a filtering operation in which the bandpass filter has an equivalent impulse response consisting of a sine wave of frequency F_c and duration 1/B. The nominal bandwidth B is defined as the inverse of the length of the input signal sample used in the correlation process. The transfer function of the filter may be found by transforming this impulse response and the power response is the square of the transfer function or

$$|H(\omega)|^2 = \frac{\sin^2((\omega-2\pi F_c)/2B)}{((\omega-2\pi F_c)/2B)^2}$$

This response function is shown in Fig. 2e. Again, B is simply the nominal bandwidth and the bandwidth between 3 dB points is about 0.89B.

Translating $|H(\omega)|^2$ down to baseband gives the power density spectrum of the signal induced component as

$$\phi_{ss}(\omega) = \frac{\sin^2(\omega/2B)}{(\omega/2B)^2} \qquad \text{(unnormalized)}$$

The normalized autocorrelation function obtained by transforming this is

$$_n\phi_{ss}(\tau) = 1 - B|\tau| \qquad 0 \leq |\tau| < 1/B$$

$$0 \qquad \text{elsewhere}$$

The limiting effective sampling rate F_s for the signal-induced component and the noise bandwidth of the filter may be obtained by integrating over $_n\phi_{ss}(\tau)$ and are equal to the nominal bandwidth B. Substituting the autocorrelation function into equation (4a) for the sampling efficiency shows that the efficiency E_s is simply F/B for sampling frequencies below B, while substitution of the spectrum into equation (4b) and recognizing that the spectral level is zero at all multiples of $\omega = 2\pi B$ shows that the efficiency equals unity whenever the sampling frequency F is an integral multiple of B. The remainder of the sampling efficiency as a function of F may be evaluated numerically using either equation (4a) or equation (4b) and is shown as the dashed curve in Fig. 7. It is interesting that

the efficiency is unity when the detector output is sampled at the rate B (that is, at intervals equal to the length of input signal being correlated with the sine wave) but drops below unity at higher sampling frequencies unless the rate is some multiple of B.

The normalized autocorrelation function ${}_n\phi_{nn}(\tau)$ for the noise-induced variance component is obtained by squaring ${}_n\phi_{ss}(\tau)$ and thus is equal to

$$
{}_n\phi_{nn}(\tau) = \begin{cases} (1 - B|\tau|)^2 & 0 \leq |\tau| < 1/B \\ 0 & \text{elsewhere} \end{cases}
$$

Integrating over this correlation function gives the limiting effective sampling rate F_n for the noise-induced component as 3B/2. Thus for a sufficiently high sampling frequency at the detector output, the noise induced component receives 3/2 as much smoothing in the averager as the signal generated component does. Inserting the correlation function into equation (4a) shows that the sampling efficiency E_n is a linear function of F up to a sampling frequency equal to B, but the efficiency for this component is only 2/3 at a sampling frequency B. Numerical evaluation of equation (4a) gives the efficiency as a function of F for higher sampling frequencies as shown by the solid curve in Fig. 7.

Physical intuition for these results can be obtained by remembering that the correlator is a transversal filter with a maximum memory time of 1/B seconds. Thus any samples of its output taken more than 1/B seconds apart are produced by totally different input data and are thus obviously uncorrelated for white noise inputs. The straight line portions E_s and E_n for sampling frequencies below B are the result of this finite memory time, and for either the signal-induced or the noise-induced component the effective sampling rate (the product of the limiting effective sampling rate F_s or F_n and the sampling efficiency E_s or E_n) is exactly equal to the actual sampling frequency F in this region. However, the finite memory length does not directly imply anything about the performance for higher sampling frequencies. For the signal-induced component, raising the sampling frequency never increases the effective sampling rate above its limit of B and, in fact, degrades performance somewhat because the correlation between samples rises faster than the sampling rate. However, the fact that the autocorrelation function is squared for the noise-induced component means that all inter-sample correlations are smaller so that additional smoothing is possible by raising the sampling frequency. Thus the effective sampling rate is not limited to the filter bandwidth B for this component, but can be raised to 3B/2 by sufficiently rapid sampling and thus provide an additional 50% of smoothing to the averager output.

CORRELATOR WITH HANNING WEIGHTING

Just as the single-tuned resonant analog filter is usually replaced by multipole filters to provide steeper skirts, the 6 dB-per-octave rolloff of the sin(x)/x frequency response function of the unweighted correlator is often found inadequate for sidelobe control. Steeper filter rolloffs can be obtained by multiplying the input data to the filter by an appropriate weighting function before correlating with the sine wave. While many weighting functions have been used for this purpose, one of the most commonly used is the function

$$W(t) = (1/2)\ (1 + \cos 2\pi Bt) \qquad 0 \leq |\tau| \leq 1/2B$$

$$0 \qquad \text{elsewhere}$$

This particular weighting function is variously referred to as Hanning weighting, raised cosine weighting, cosine-squared weighting, or sine-squared weighting. One of the desirable properties of this weighting function is what W(t) and its derivitive are both continuous over and beyond the correlation interval and that the first discontinuity appears in the second derivitive. This gives a filter rolloff of 18 dB-per-octave and greatly reduces sidelobes or spillover from one spectrum analyzer channel to another.

A second desirable property of the Hanning function is that it has a simple Fourier transform and thus can be implemented at the output of a spectrum analyzer using an unweighted correlator. The equivalent of the Hanning weighting function is obtained by adding together the output of the correlator in the desired frequency bin and the average of the outputs of the two adjacent bins, if the frequency interval between the bins is equal to B. Either approach, weighting the data before correlating or adding together frequency bins after spectrum analysis, yields a filter power response given by

$$|H(\omega)|^2 = \frac{\sin^2((\omega-2\pi F_c)/2B)}{((\omega-2\pi F_c)/2B)^2}\left[\frac{1}{1-((\omega-2\pi F_c)/2\pi B)^2}\right]^2$$

This power response is shown in Fig. 2f. Note that the central peak is broadened relative to that of the unweighted correlator so that the 3 dB bandwidth is about 1.4 B, and that the first zero in the response is separated from the center frequency by 2B. The sidelobes of the response are not shown in Fig. 2f, but the first is about 31.5 dB below the central peak and they fall off at 18 dB-per-octave as the separation from the central peak increases. Translating $|H(\omega)|^2$ to baseband to obtain the power density spectrum of the signal-induced detector variance gives a spectrum

$$\Phi_{ss}(\omega) = \frac{\sin^2(\omega/2B)}{(\omega/2B)^2}\left[\frac{1}{1-(\omega/2\pi B)^2}\right]^2 \qquad \text{(unnormalized)}$$

and a corresponding normalized autocorrelation function of

$$n\phi_{ss}(\tau) = (1/3)(2+\cos(2\pi B\tau))(1-B\tau) + (1/2\pi)\sin(2\pi B\tau) \quad \text{for } |\tau| < 1/B$$

$$0 \qquad \text{elsewhere}$$

Integrating over this correlation function and using equation (3a) gives the noise bandwidth and F_s for the signal-induced component as 3B/2. Thus the noise bandwidth of the Hanning weighted filter is increased by 50% relative to the unweighted system. This agrees with the expected increase in the variance produced by adding the adjacent bins at half amplitude, assuming the fluctuations in these adjacent bins are uncorrelated with those in the central bin.

The value F_n of the limiting effective sampling rate for the noise-induced component of the detector variance is obtained by integrating the square of $n\phi_{ss}(\tau)$ and is given by

$$F_n = \frac{24\pi^2 B}{8\pi^2 + 35}$$

or about 2.08 B. Evaluation of the efficiency E_s or E_n for each of the variance components is best done numerically using equation (4a) and using $n\phi_{ss}(\tau)$ for the signal-induced component and $n\phi_{nn}(\tau) = n\phi_{ss}^2(\tau)$ $n\phi_{ss}(\tau)$ for the noise-induced component. Again, because of the finite extent of the correlation function, the efficiencies are directly proportional to F for sampling frequencies below the nominal bandwidth B, and the effective sampling rate in this region is just equal to the actual sampling frequency. As shown in Fig. 8, the sampling efficiencies continue to follow the asymptotes closely until E_s or E_n reaches about .9 and then bend sharply toward the limit of unity. Thus, while the sampling efficiencies are about 48% and 67% respectively for the noise-induced and the signal-induced components when sampling is done at the nominal filter bandwidth B, these efficiencies rise to about 91% and nearly 100% respectively when the sampling frequency at the detector output is doubled.

CONCLUSIONS

The sampling efficiency curves shown in Figs. 3 through 8 for various filter functions indicate that the effective smoothing obtained by averaging sampled outputs of a narrow band detector is a complex function of the sampling frequency used. In order to determine the smoothing obtained it is necessary to separate the output fluctuations of the detector into two components, one induced by noise alone at the narrow band filter input and the other induced by any signal present in the noise. The ultimate amount of smoothing available for each of these two components with very high sampling rates is described by the effective sampling rates F_s and F_n shown for each filter function in Table 1. In general, these two limiting rates are unequal and differ from the nominal bandwidths of the narrow band filters.

The sampling efficiency curves indicate that the effective sampling rate may be significantly less than the ultimate value when the averager input is sampled at a rate comparable to the nominal filter bandwidth, as is often done in practice. A reduction in sampling efficiency may be equated to a similar shortening of the averaging time in its effect on the smoothing of the output so that, for example, a 50% sampling efficiency doubles the output variance of the averager just as would occur if the averaging time were cut in half. If a particular ratio of mean squared output to variance is required for detection of a signal, it can be shown that the signal level must be increased by 5 log (1/E) decibels to compensate for the loss of smoothing. Since the sampling efficiencies (particularly for the noise-induced component which is important in false alarm rate determination) typically lie in the 0.4 to 0.8 range when the detector is sampled at a rate equal to the nominal bandwidth B of the narrow band filter, losses on the order of one to two decibels of potential signal sensitivity at the system input may be experienced due to this effect. The cure is to design the system to sample the detector output at a higher frequency in order to bring the sampling efficiency closer to unity. The amount of increase necessary depends on the amount of loss considered acceptable and on the filter bandpass function. In general, filters with steeper skirts such as the third-order Butterworth and the Hanning weighted correlator approach their ultimate performance with lower sampling rates than do filters with weaker sidelobe control.

Filter Type	Power Response Function ($dF = \omega/2\pi - F_c$)	Noise Bandwidth (single sided)	3 db Bandwidth	F_s (for signal induced term)	F_n (for noise induced term)
Ideal Bandpass	1 $\lvert dF \rvert < B/2$ 0 $\lvert dF \rvert > B/2$	B	B	B	B
Single Tuned Circuit	$\frac{(B/2)^2}{(B/2)^2 + dF^2}$	$\pi B/2$ =1.57 B	B	$\pi B/2$ =1.57 B	πB =3.14 B
Third Order Butterworth	$\frac{(B/2)^6}{(B/2)^6 + dF^6}$	$\pi B/3$ =1.05 B	B	$\pi B/3$ =1.05B	$2\pi B/5$ =1.26 B
Gaussian	$\exp(-(dF/B)^2)$	$\sqrt{\pi}B$ =1.77 B	1.67 B	$\sqrt{\pi}B$ =1.77 B	$\sqrt{2\pi}B$ =2.51 B
Unweighted Correlator	$\frac{\sin^2(\pi dF/B)}{(\pi dF/B)^2}$	B	.89 B	B	3B/2 =1.5 B
Hanning Weighted Correlator	$\left[\frac{\sin^2(\pi dF/B)}{(\pi dF/B)^2}\right] \cdot \left[\frac{1}{(1-(dF/B)^2)^2}\right]$	3B/2 =1.5 B	1.42 B	3B/2 =1.5 B	$\frac{24\pi^2 B}{8\pi^2 + 35}$ =2.08 B

Table 1. Parameters of Various Bandpass Filter Functions

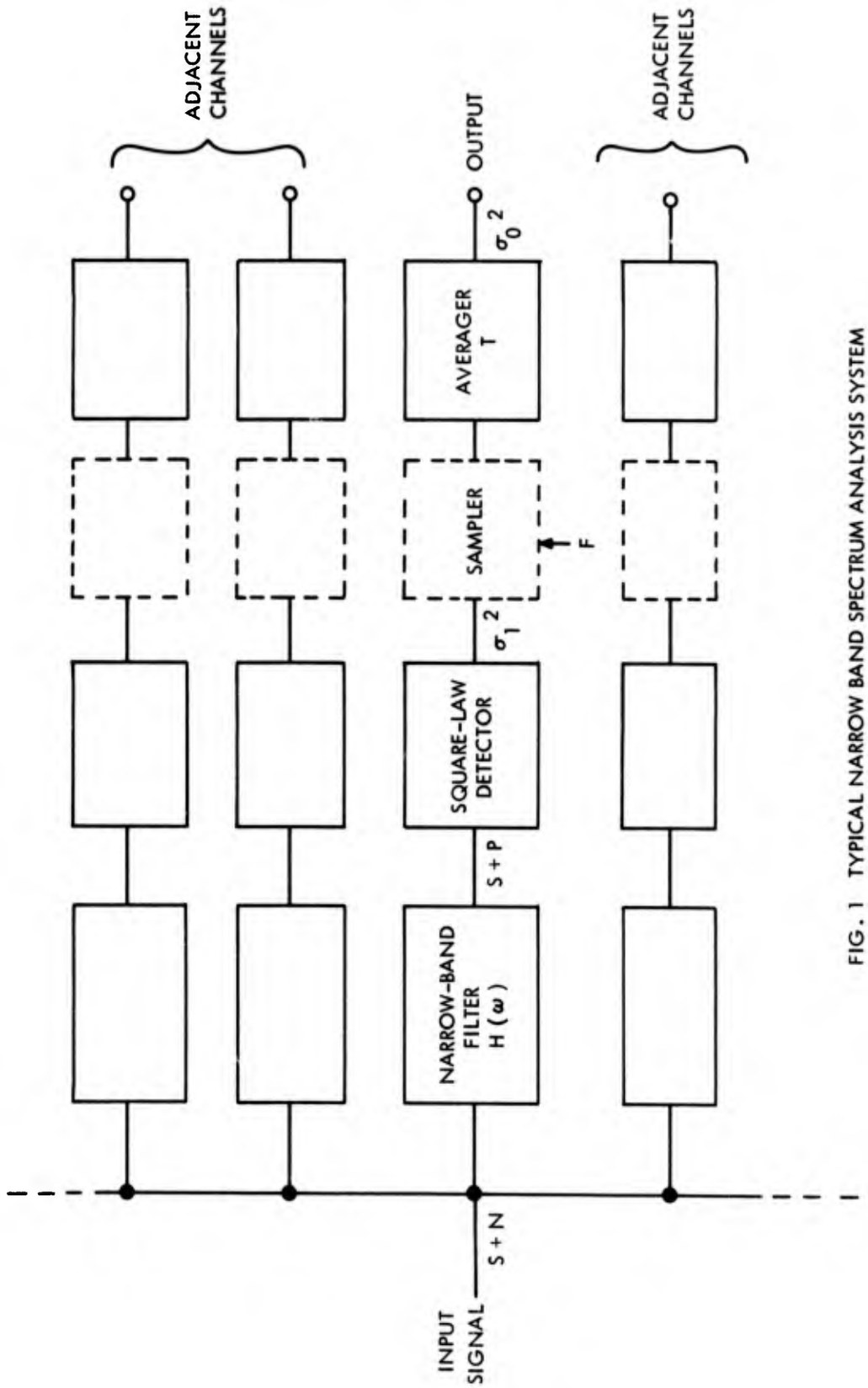

FIG. 1 TYPICAL NARROW BAND SPECTRUM ANALYSIS SYSTEM

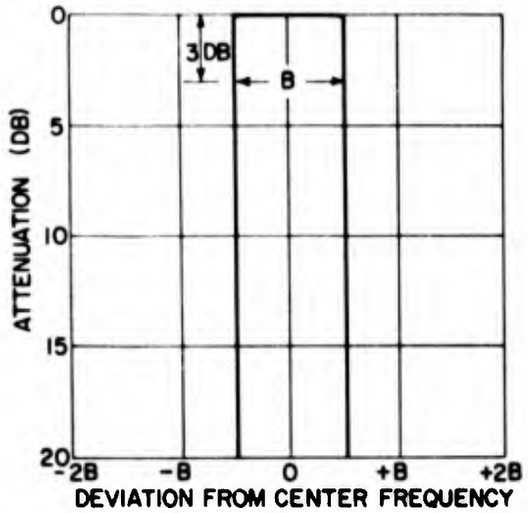

FIG. 2a RESPONSE OF IDEAL BANDPASS FILTER

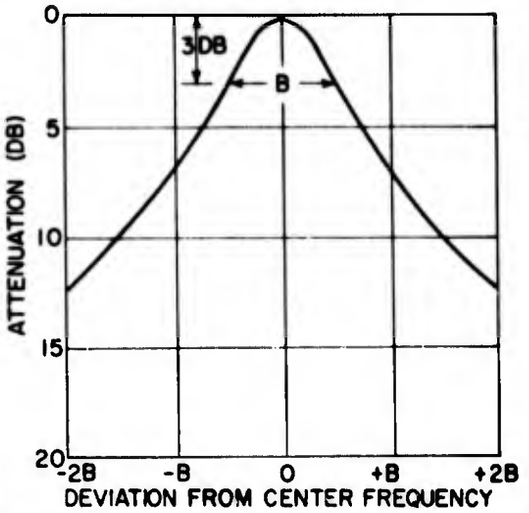

FIG. 2b RESPONSE OF SINGLE TUNED FILTER

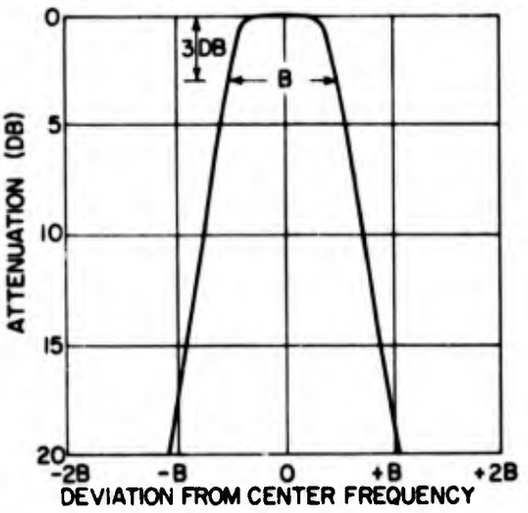

FIG. 2c RESPONSE OF 3RD ORDER BUTTERWORTH FILTER

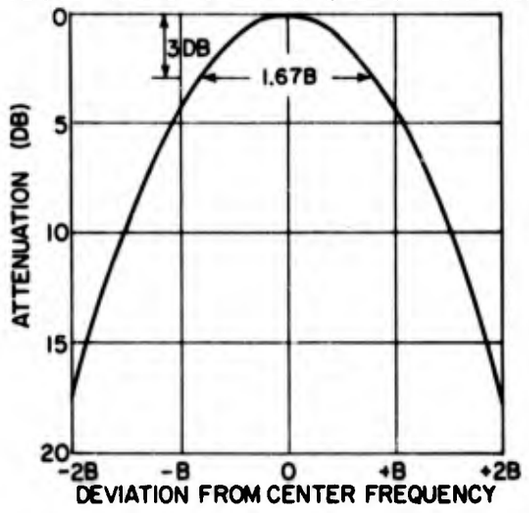

FIG. 2d RESPONSE OF GAUSSIAN FILTER

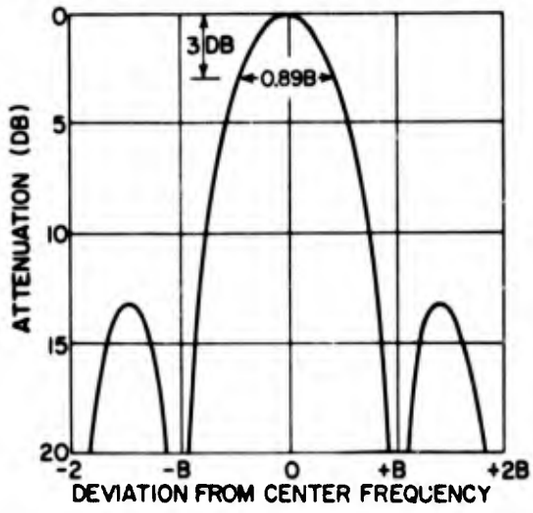

FIG. 2e RESPONSE OF UNWEIGHTED CORRELATOR

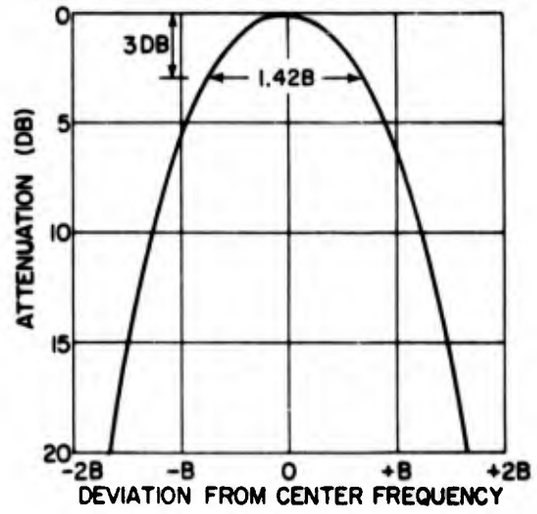

FIG. 2f RESPONSE OF HANNING WEIGHTED CORRELATOR

FIG. 2 FREQUENCY RESPONSE OF VARIOUS BANDPASS FILTERS

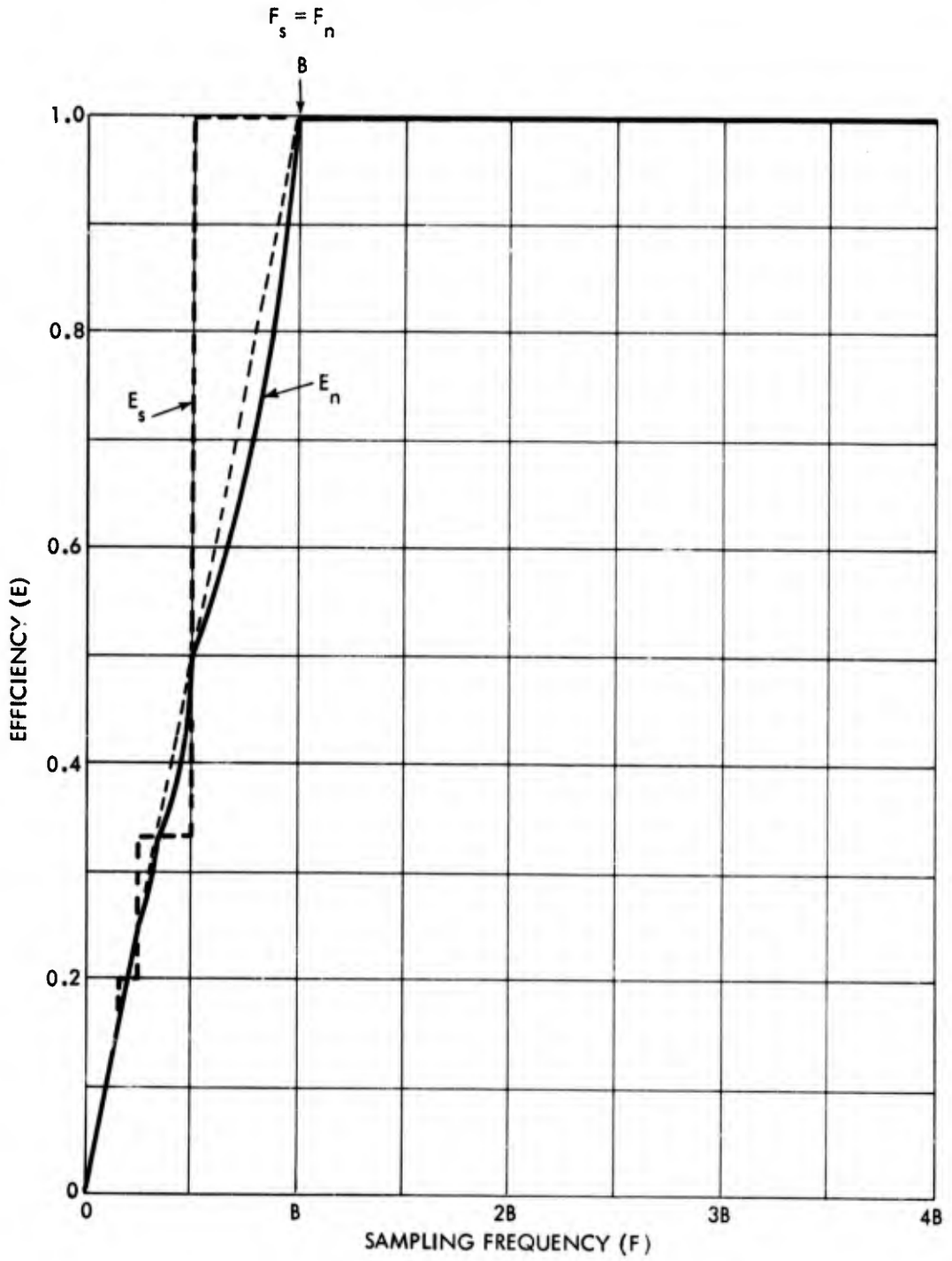

FIG. 3 SAMPLING EFFICIENCY FOR IDEAL BANDPASS FILTER

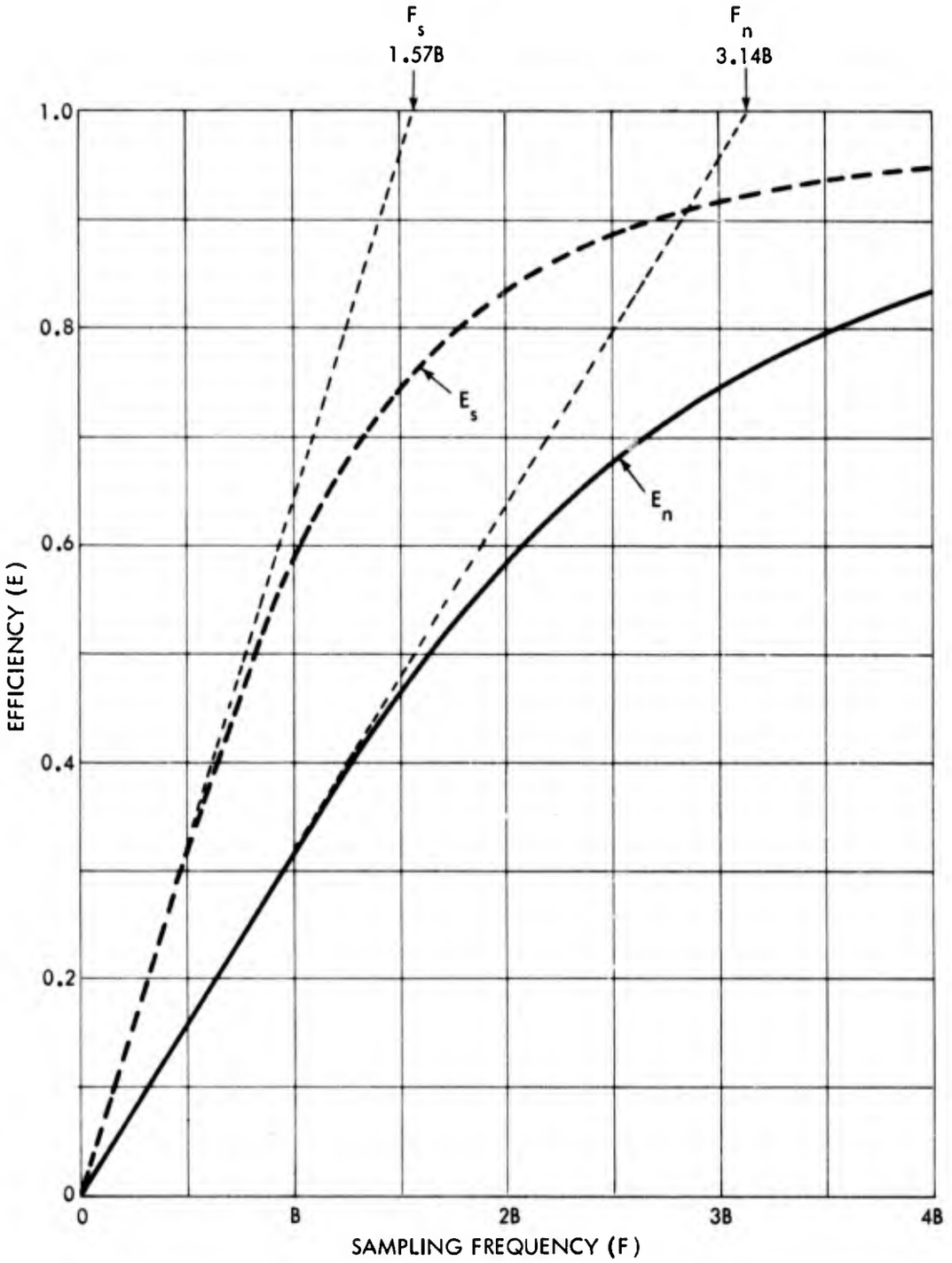

FIG. 4 SAMPLING EFFICIENCY FOR SINGLE-TUNED RESONANT FILTER

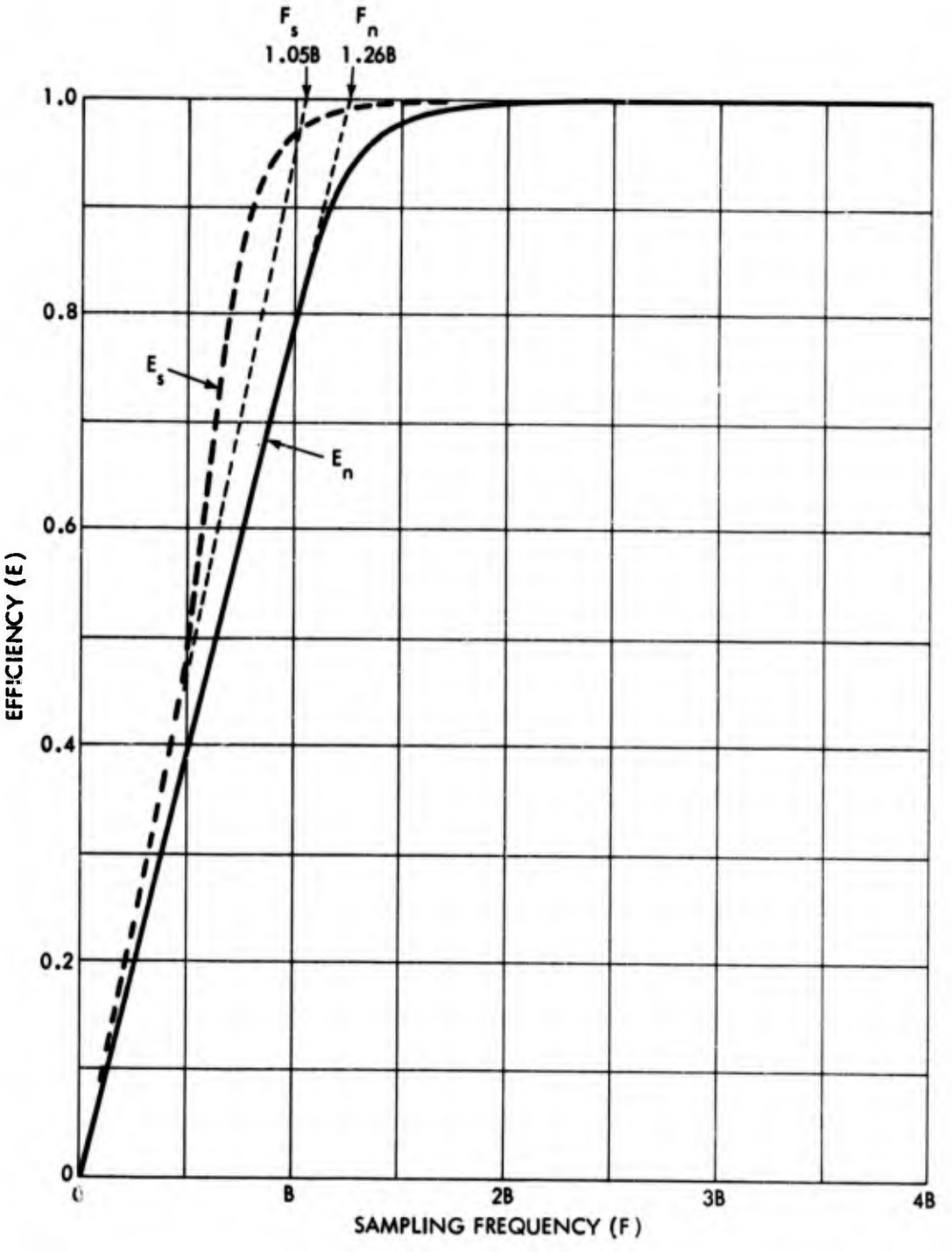

FIG. 5 SAMPLING EFFICIENCY FOR THIRD-ORDER BUTTERWORTH FILTER

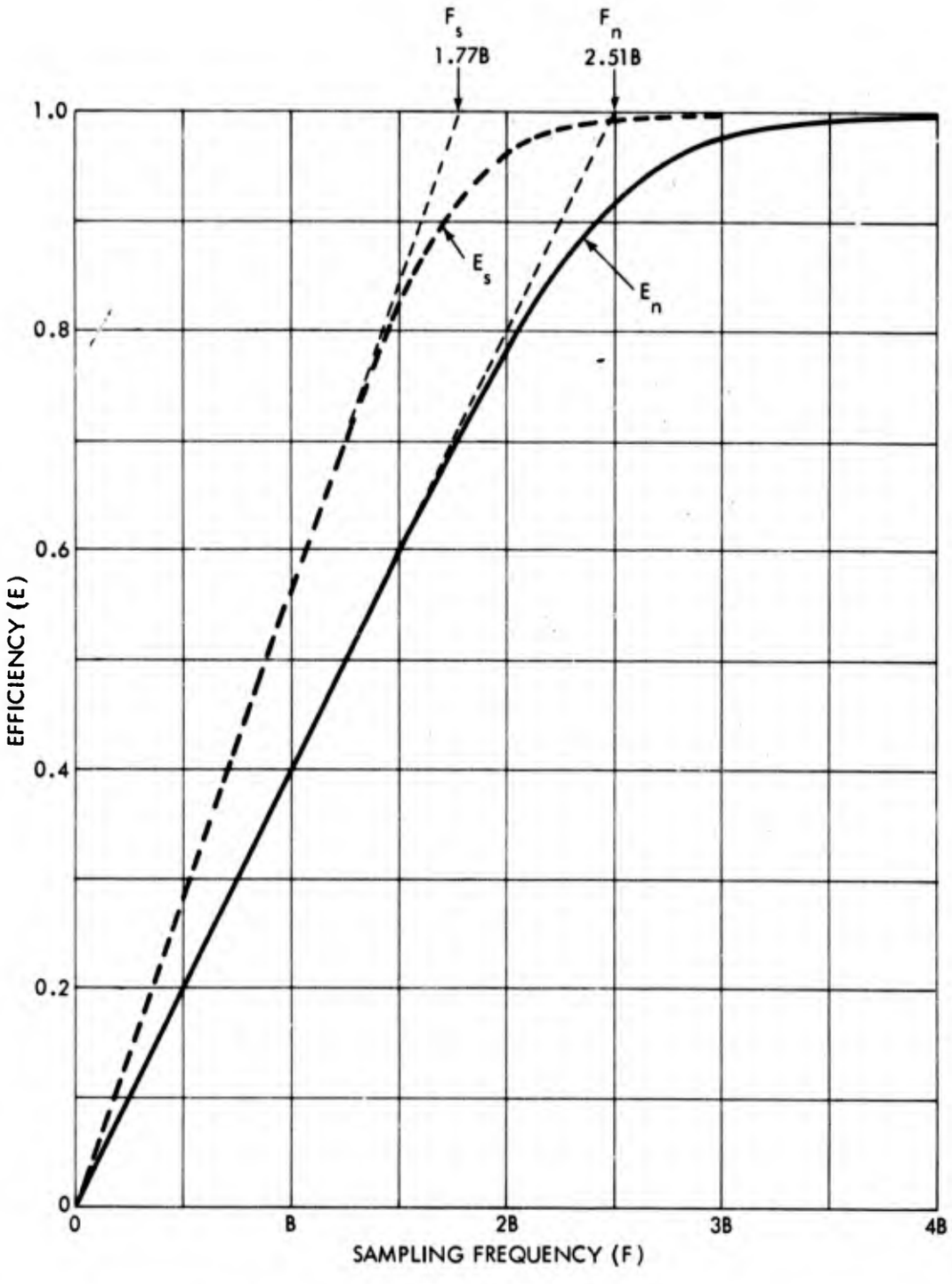

FIG. 6 SAMPLING EFFICIENCY FOR GAUSSIAN FILTER

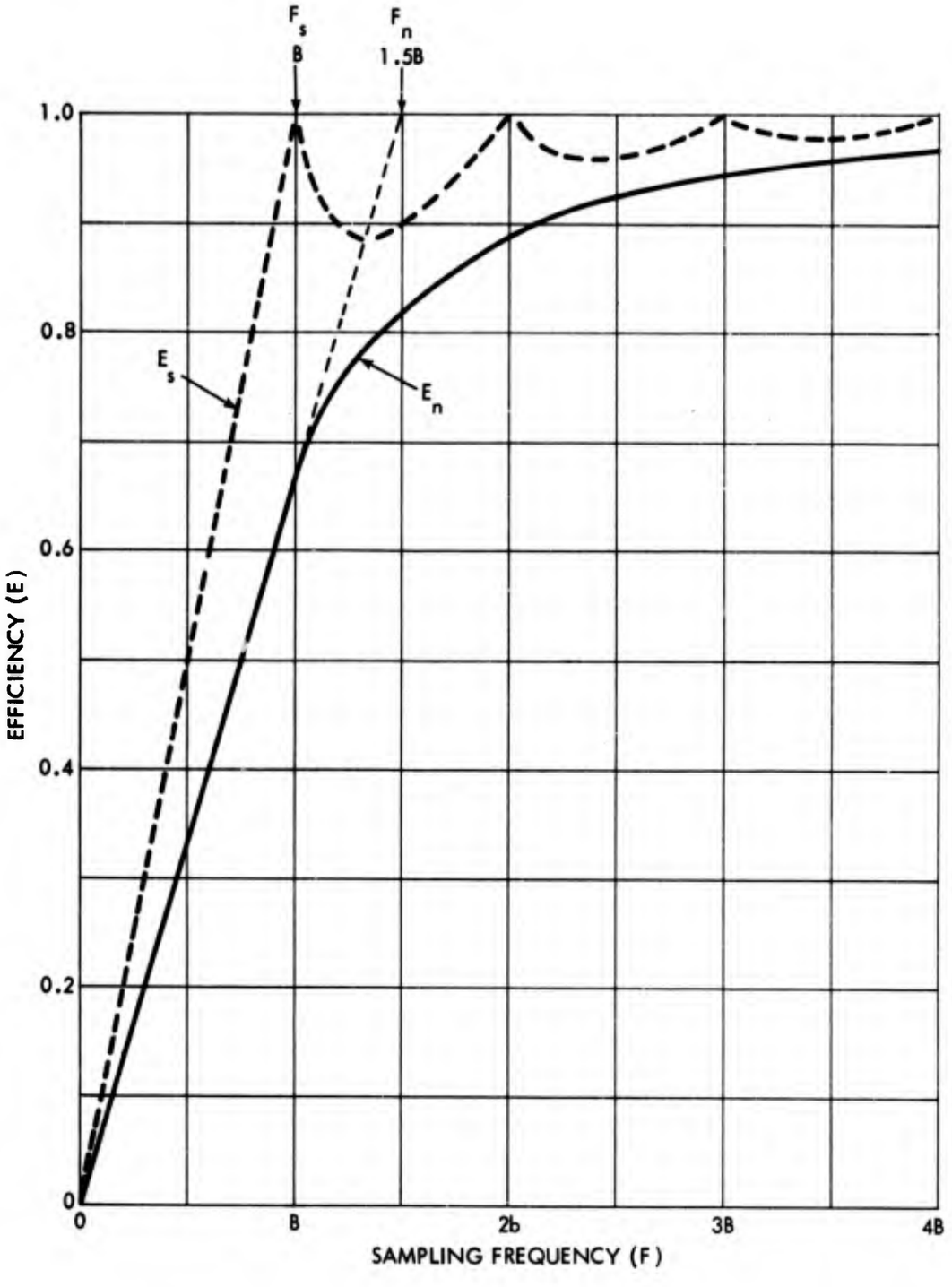

FIG. 7 SAMPLING EFFICIENCY FOR UNWEIGHTED CORRELATOR

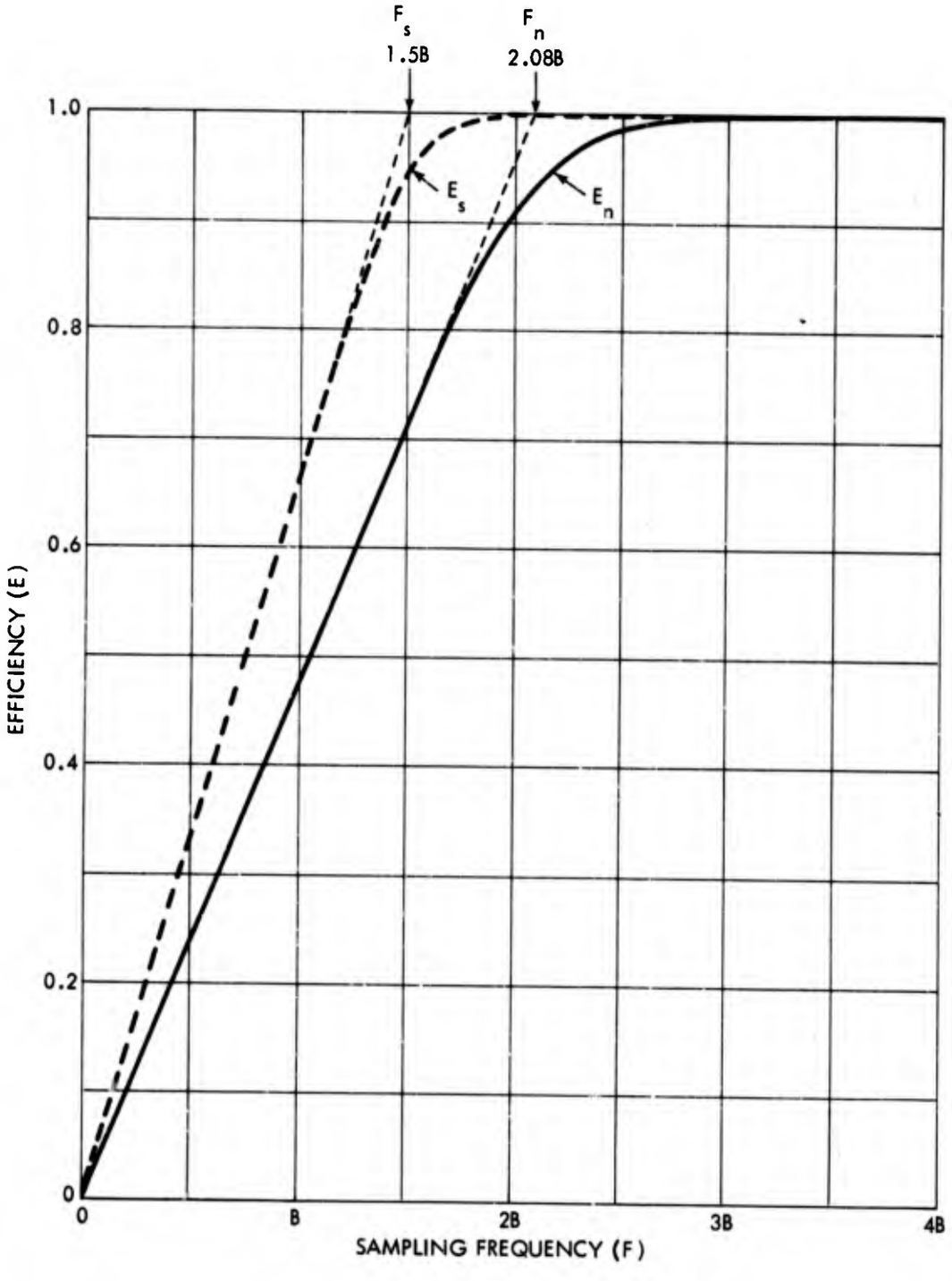

FIG. 8 SAMPLING EFFICIENCY FOR HANNING WEIGHTED CORRELATOR

APPENDIX A

THE EFFECT OF FINITE SAMPLING RATES ON A TIME-AVERAGING SYSTEM

The contents of this Appendix originally appeared in an internal Naval Ordnance Laboratory report (NOLTN 5209) dated 25 April 1961. Minor changes have been made in notation, and in particular the factor $1/2\pi$ has been moved to the inverse Fourier transform rather than the forward transform in equations (A6a) and (A6b) and those following to conform with the more common notation.

The Nyquist sampling rate theorem states that a band-limited signal with no frequency components above a frequency F_{max} may be sampled at a frequency greater than or equal to $2F_{max}$ and then reconstructed exactly from these samples if certain ideal conditions are allowed for the reconstruction procedure. This implies that all the information contained in the original signal is contained in its samples so that any sort of data reduction process can work with the sampled signal as well as with the original signal with no sacrifice in performance. When the signal is not band-limited, no finite sampling frequency will preserve all the information. However, in many data processing situations it is still necessary to use sampled information and it is useful to ask how system performance is affected by finite sampling rates.

This can be studied for a simple (and fairly general) sort of data processing system which simply generates the time average of a random input signal, averaging over the last T seconds. The output variance (noise power) of this averaging device is studied as the input signal is sampled at various sampling frequencies. (See Figure A-1.) This output variance has been found by J. P. Costas (references A1 and A2) to be

$$\sigma_o^2 = \frac{1}{N} \sum_{K=-N}^{N} \left(1 - \frac{|K|}{N}\right) \phi_{ii} \left(\frac{K}{F}\right) \sigma_i^2 \qquad \text{(A1)}$$

where $\phi_{ii}(\tau)$ is the autocorrelation function of the normalized input signal (that is with the mean subtracted out and divided by its rms value so that $\phi_{ii}(o)$ equals one and $\phi_{ii}(\tau)$ approaches zero as τ approaches infinity). F is the frequency at which samples are taken and $N = FT$ is the number of samples taken during the T second interval. If the samples were independent $\phi_{ii}(K/F)$ would be one for $K = 0$ and zero for all other K. Thus the output variance would reduce to σ_i^2/N.

We can now write the output variance obtained in equation (A1) in terms of a quantity N_{eT}, defined as the effective number of independent samples which must be taken during the interval T in order to produce the same output variance. Thus

$$\frac{\sigma_i^2}{N_{eT}} = \sigma_o^2 = \frac{1}{N} \sum_{K=-N}^{N} \left(1 - \frac{|K|}{N}\right) \phi_{11} \left(\frac{K}{F}\right) \sigma_i^2$$

or

$$N_{eT} \triangleq \frac{N}{\sum_{K=-N}^{N} \left(1-\frac{|K|}{N}\right) \phi_{11} \left(\frac{K}{F}\right)} \tag{A2}$$

Thus N_{eT} may be interpreted as the effective number of independent samples (or measurements) obtained from the input signal for the purpose of generating an average in T seconds, based on the variance of the output. Since the number of samples in the time T is FT, we can define an effective average sampling frequency during the time interval T as $F_{eT} = (N_{eT}/T)$. We can thus write for the effective average frequency of independent samples.

$$F_{eT} \triangleq \frac{F}{\sum_{K=-FT}^{FT} \left(1-\frac{|K|}{FT}\right) \phi_{11} \left(\frac{K}{F}\right)} \tag{A3}$$

Provided that $\sum_{K=1}^{n} K\phi_{11}\left(\frac{K}{F}\right)$ has a finite limit as n approaches infinity a limit will exist for F_{eT} as T approaches infinity. This condition will hold as long as the power density spectrum of the input signal has no more than a finite number of step discontinuities and no discontinuities worse than steps. Thus we can write

$$F_e \triangleq \lim_{T\to\infty} F_{eT} = \frac{F}{\sum_{K=-\infty}^{\infty} \phi_{11}\left(\frac{K}{F}\right)} \tag{A4}$$

F_e is thus the effective frequency of independent samples for long averaging periods and this limit is approached rather rapidly when the averaging period is appreciably greater than the width of the autocorrelation function.

A philosophical argument may also be used to justify this limit. The first sample in the interval T may be thought of as unconstrained while the following samples are correlated with those preceding and therefore contain less new information. After a sufficiently long train of samples is taken that they are no longer correlated with the first sample, the amount of new information per sample becomes constant. Thus the average information per sample reaches a limiting value when the train of samples is long compared to the correlogram width and this is what is being computed in equation (A4).

Thus from equation (A4) we are able to compute the effective frequency at which independent samples appear to occur, based on the output variance of the averaging system, as a function of the actual sampling frequency. If the sampling frequency is increased indefinitely, the output variance is not reduced below a certain value, so there is a limiting value to the effective frequency of independent samples which may be obtained from the input signal. This is given by

$$F_o \triangleq \lim_{F\to\infty} F_e = \frac{1}{\int_{-\infty}^{\infty} \phi_{11}(\tau)\, d\tau} \qquad \text{(A5)}$$

Thus F_o may be thought of as the maximum frequency at which it is possible to extract information (in the form of independent samples for an averaging measurement) from the input signal while F_e is the effective frequency of independent samples when some finite actual sampling frequency is used. A study of F_e as a function of F and its value relative to F_o thus displays the effect of finite sampling frequencies on the performance of the averaging system, and may therefore be used to determine required sampling rates for given input signals.

It is often more convenient to work with the frequency power density spectrum of an input signal than with its autocorrelation function and we may write expressions equivalent to equations (A4) and (A5) in the frequency domain by making use of the transform pair:

$$\Phi_{11}(\omega) = \int_{-\infty}^{\infty} \phi_{11}(\tau) e^{-j\omega\tau} d\tau \qquad \text{(A6a)}$$

$$\phi_{11}(\tau) = \frac{1}{2\pi} \int_{-\infty}^{\infty} \Phi_{11}(\omega) e^{j\omega\tau} d\omega \qquad \text{(A6b)}$$

where $\phi_{11}(\omega)$ is the normalized power density spectrum of the input. Notice that we may express in integral form the sum

$$\sum_{K=-\infty}^{\infty} \phi_{11}\left(\frac{K}{F}\right) = \int_{-\infty}^{\infty} m(\tau)\ \phi_{11}(\tau)d\tau \tag{A7}$$

where $m(\tau)$ is a train of impulses and may be written either as a sum of impulses or as the sum of its complex Fourier components

$$m(\tau) = \sum_{K=-\infty}^{\infty} \delta\left(\tau-\frac{K}{F}\right) = F \sum_{n=-\infty}^{\infty} e^{-j2n\pi F\tau} \tag{A8}$$

Inserting the latter form for $m(\tau)$ into equation (A7) yields for the sum

$$\sum_{K=-\infty}^{\infty} \phi_{11}\left(\frac{K}{F}\right) = \int_{-\infty}^{\infty} \phi_{11}(\tau) \left[F \sum_{n=-\infty}^{\infty} e^{-j2n\pi F\tau}\right] d\tau \tag{A9a}$$

Or by exchanging the order of summation and integration

$$\sum_{K=-\infty}^{\infty} \phi_{11}\left(\frac{K}{F}\right) = F \sum_{n=-\infty}^{\infty} \int_{-\infty}^{\infty} \phi_{11}(\tau)e^{-j2n\pi F\tau}d\tau \tag{A9b}$$

The integral in equation (A9b) may now be recognized as the Fourier transform form of $\phi_{11}(2n\pi F)$, so we may finally write the sum of the samples of the time function as the sum of samples of a frequency function:

$$\sum_{K=-\infty}^{\infty} \phi_{11}\left(\frac{K}{F}\right) = F \sum_{n=-\infty}^{\infty} \phi_{11}(2n\pi F) \tag{A10}$$

and equation (A4) may be rewritten as

$$F_e = \frac{1}{\sum_{n=-\infty}^{\infty} \phi_{11}(2n\pi F)} \tag{A11}$$

Similarly the denominator of equation (A5) may be recognized as equivalent to (A6a) with ω equal to zero, so that

$$F_o = \frac{1}{\phi_{11}(0)} \tag{A12}$$

Thus F_e and F_o may each be written in two different forms, one pertaining to the time domain (autocorrelation function) and the other to the frequency domain (power density spectrum). From equations (A11) and (A12) and the non-negative property of $\phi_{11}(\omega)$, it is clear that F_e for any finite sampling frequency cannot exceed F_o.

Summarizing, the effective frequency of occurrence of independent samples (that is, the frequency at which independent samples must be taken to provide the same output variance in an averaging device) for a given actual sampling frequency F is given by

$$F_e = \frac{F}{\sum_{K=-\infty}^{\infty} \phi_{11}\left(\frac{K}{F}\right)} \tag{A4}$$

or

$$F_e = \frac{1}{\sum_{n=-\infty}^{\infty} \phi_{11}(2n\pi F)} \tag{A11}$$

And the maximum effective frequency of independent samples when the actual sampling frequency is increased indefinitely is given by either

$$F_o = \frac{1}{\int_{-\infty}^{\infty} \phi_{11}(\tau)\, d\tau} \tag{A5}$$

or

$$F_o = \frac{1}{\phi_{11}(0)} \tag{A12}$$

It should be emphasized at this point that F_o is simply the maximum frequency at which independent sample points can be extracted from the input signal for the purpose of averaging when an infinite actual sampling frequency is used. It is not necessarily true that this effective rate can be realized by choosing the actual sampling frequency to be F_o as will be shown by the examples. F_o is, however, a reasonable measure of the bandwidth of the signal from an information-carrying point of view and F_e for a finite sampling frequency gives an indication of the amount of information lost in the sampling process.

Formulas similar to equations (A5) and (A12) are given in a paper by McPherson (reference (A3)) and attributed to Sherwin (reference (A4)) for the "equivalent rate of independent samples per unit time" in a continuous noise signal. This is interpreted by McPherson to be twice the "white noise bandwidth" of the noise signal where the latter is defined as the cutoff frequency of a band-limited noise signal with the same power density at zero frequency and the same total power as the given noise signal.

EXAMPLES:

1. Rectangular Wave with Poisson Distributed Zero-Crossings.

The autocorrelation function for a signal which is either plus or minus one volt and has zero-crossings Poisson distributed at an average frequency α, is (reference (A5)):

$$\phi_{11}(\tau) = e^{-2\alpha|\tau|} \qquad \text{all } \tau$$

Using equation (A5) we can compute the effective frequency F_o of independent samples for an infinite sampling rate.

$$F_o = \frac{1}{\int_{-\infty}^{\infty} e^{-\alpha|\tau|}\,d\tau} = \frac{1}{2\int_{0}^{\infty} e^{-2\alpha\tau}\,d\tau} = \frac{1}{2\left(\frac{1}{2\alpha}\right)} = \alpha$$

Also, using equation (A4) directly, the effective sampling frequency F_e may be found as a function of the actual sampling rate F as:

$$F_e = \frac{F}{\sum_{K=-\infty}^{\infty} e^{-2\alpha\frac{|K|}{F}}} = \frac{F}{1+2\sum_{K=1}^{\infty} e^{-2\alpha\frac{K}{F}}} = \frac{F}{1+2\frac{e^{-2\alpha/F}}{1-e^{-2\alpha/F}}} = F\,\frac{1-e^{-2\alpha/F}}{1+e^{-2\alpha/F}}$$

This function is plotted in Figure A2 and approaches F_o asymptotically as F increases. The function never quite reaches F_o because of the infinite range of frequencies in the input signal, but it gets fairly close for sampling frequencies appreciably above F_o. For example, if F_o is chosen as the actual sampling frequency, the effective sampling frequency will only be 0.762 F_o so about 24% of the available input information is lost in this case. Doubling the actual sampling frequency to 2 F_o gives an effective sampling rate of 0.924 F_o, so the information lost in sampling is reduced to 7.6%.

2. Ideal Band-Limited Signal

A signal with a flat spectrum band-limited at a radian frequency ω_o has normalized autocorrelation function given by:

$$\phi_{11}(\tau) = \frac{\sin\omega_o\tau}{\omega_o\tau} \quad \text{all } \tau$$

and a spectrum given by:

$$\phi_{11}(\omega) = \frac{\pi}{\omega_o} \qquad |\omega| < \omega_o$$

$$= \frac{\pi}{2\omega_o} \qquad \omega = \pm\omega_o$$

$$= 0 \qquad |\omega| > \omega_o$$

F_o may be found easily either by equation (A5) or equation (A12) and is ω_o/π or twice the cutoff frequency in Hertz. Thus the rate at which independent samples appear to occur given an infinite sampling rate is just the Nyquist rate as given by the usual sampling theorem.

It is not easy to find an expression for F_e in the time domain, so equation (A11) is used for this, taking advantage of the simple form of the spectrum. The result, obtained simply by counting the number of values of n for which $2\pi nF$ has a value smaller than ω_o is:

$$F_e = \frac{\omega_o}{(2n+1)\pi} \quad \frac{\omega_o}{2n\pi} > F > \frac{\omega_o}{(2n+2)\pi} \qquad n = 0, 1, 2, \ldots$$

$$F_e = \frac{\omega_o}{2n\pi} \qquad F = \frac{\omega_o}{2n\pi} \qquad n = 1, 2, 3, \ldots$$

This function is plotted in Figure A3. Roughly, the effective sampling frequency follows the actual sampling frequency by oscillating in steps about it up to F_o, then remains at F_o as the actual sampling frequency is increased. This differs from the previous example in that there is a sampling frequency above which no increase in effective sampling frequency is observed as would be expected from the sampling theorem.

A striking characteristic of this function is that the effective sampling frequency can exceed the actual sampling frequency in some cases, due to the tendency for the noise components to cancel each other in consecutive samples. Thus any sampling frequency above one-half the Nyquist frequency will give the same performance (output noise) as independent samples occurring at the Nyquist frequency.

3. Clipped Ideal Band-Limited Signal

If a signal with a flat spectrum and Gaussian distribution of amplitudes is band-limited at a frequency ω_o and then subjected to extreme amplification and clipping (reduced to polarity-only information) the autocorrelation function of the resulting signal will be (reference (A6)):

$$\phi_{11}(\tau) = \frac{2}{\pi} \arcsin \frac{\sin\omega_o\tau}{\omega_o\tau} \qquad \text{all } \tau$$

For purposes of analysis this autocorrelation function may be broken up into the sum of two functions, thus:

$$\phi_{11}(\tau) = \phi_{aa}(\tau) + \phi_{bb}(\tau) = \frac{2}{\pi} \frac{\sin\omega_o\tau}{\omega_o\tau} + \frac{2}{\pi}\left[\arcsin\frac{\sin\omega_o\tau}{\omega_o\tau} - \frac{\sin\omega_o\tau}{\omega_o\tau}\right]$$

The effective frequency of independent samples may now be obtained from equation (A5), integrating the correlation function in its two parts. The first term may be integrated analytically and the second is essentially zero for all values of its argument above π/ω_o (see Fig. A4) and may therefore be handled numerically. The integral of the first term is $2/\omega_o$ and the integral of the second is approximately $0.523/\omega_o$. Thus F_o is approximately $\omega_o/2.523$ or approximately 1.24 times greater than that for the unclipped signal of example 2.

F_e must be evaluated rather indirectly by using equation (A10) and the results of example 2 to find

$$\sum_{K=-\infty}^{\infty} \phi_{aa}\left(\frac{K}{F}\right)$$

and numerical techniques to find

$\sum_{K=-\infty}^{\infty} \phi_{bb}(\frac{K}{F})$. Thus for the first term

$$\sum_{K=-\infty}^{\infty} \phi_{aa}(\frac{K}{F}) = \frac{2}{\pi} \sum_{K=-\infty}^{\infty} \frac{\sin\omega_o(K/F)}{\omega_o(K/F)} = \frac{2}{\pi} \frac{F}{2F_e}$$

where $_2F_e$ is the F_e computed in example 2. Thus

$$\sum_{K=-\infty}^{\infty} \phi_{aa}(\frac{K}{F}) = \frac{2(2n+1)F}{\omega_o} \quad \frac{\omega_o}{2n\pi} > F > \frac{\omega_o}{(2n+2)\pi} \quad n = 0, 1, 2, \ldots$$

$$= \frac{4nF}{\omega_o} \quad F = \frac{\omega_o}{2n\pi} \quad n = 1, 2, 3, \ldots$$

The second term $\sum_{K=-\infty}^{\infty} \phi_{bb}(\frac{K}{F})$

is computed numerically and is plotted in Fig. A5. For sampling frequencies below ω_o/π it is constant at 0.364 and for high sampling frequencies it approaches the assymptote $0.523\ F/\omega_o$.

By adding the two terms of the correlogram after summing we can now evaluate F_e by means of equation (A4). For sampling frequencies below $\omega_o/2\pi$ we can make use of the constant value of the second term and write:

$$F_e = \frac{F}{\sum_{K=-\infty}^{\infty} \phi_{aa}(\frac{K}{F}) + \sum_{K=-\infty}^{\infty} \phi_{bb}(\frac{K}{F})}$$

$$= \frac{F}{\frac{2(2n+1)F}{\omega_o} + 0.364} \quad \frac{\omega_o}{2n\pi} > F > \frac{\omega_o}{(2n+2)\pi} \quad n = 1, 2, 3, \ldots$$

$$= \frac{F}{\frac{4nF}{\omega_o} + 0.364} \qquad F = \frac{\omega_o}{2n\pi} \qquad n = 1, 2, 3, \ldots$$

while for frequencies above $\omega_o/2\pi$ the first term is constant and we may write F_e as

$$F_e = \frac{F}{\frac{2F}{\omega_o} + \sum_{K=-\infty}^{\infty} \phi_{bb}(\frac{K}{F})} \qquad F > \frac{\omega_o}{2\pi}$$

where $\sum_{K=-\infty}^{\infty} \phi_{bb}(\frac{K}{F})$ is taken from the plot in Fig. A5. For frequencies sufficiently high that $\sum_{K=-\infty}^{\infty} \phi_{bb}(\frac{K}{F})$ approaches its assymptotic value $0.523\ F/\omega_o$, the value of F_e approaches its maximum value of F_o. The functional relationship of F_e with the actual sampling frequency F is shown in Figure A6. Again, as in example 2, the effective sampling frequency tends to change in steps as the actual sampling frequency is increased. However, for the clipped signal the effective sampling frequency never reaches the F_o for any finite actual sampling frequency, so it is no longer possible to extract all the available information from the signal by sampling at the Nyquist rate ω_o/π. The reason is that the signal after clipping is no longer band-limited so that sampling at a higher frequency provides more information for averaging. The proper interpretation of this is certainly not that clipping increases the information content, but that sampling the clipped signal at a frequency above the Nyquist frequency helps to remove the noise introduced by clipping. Thus an increase in effective sampling frequency by a factor of 1.24 is possible by extreme oversampling and most of this is gained by sampling at about three times the Nyquist frequency.

REFERENCES - APPENDIX A

(A1) Costas, J. P., Periodic Sampling of Stationary Time Series, Technical Report #156, Research Laboratory of Electronics, MIT (1950).

(A2) Lee, Y. W., Statistical Theory of Communication, Chapter II, J. Wiley & Sons, Inc. (1960)

(A3) McPherson, R. R., On a Formula for Equivalent Number of Noise Samples Per Unit Time, Technical Memorandum #35, Univ. of Michigan, Dept. of Electrical Engineering Defense Group, Jan. 1957.

(A4) Sherwin, C. W., Detection of Pulsed Signals With a Narrow-Band Filter, Detector, and Integrator, Report R-42, Control Systems Laboratory, University of Illinois, 15 June 1953.

(A5) Lee, Y. W., op. cit.
(A6) VanVleck, J. H., The Spectrum of Clipped Noise, Report #51, pp. 23-24, Radio Research Laboratory Harvard University, 21 July 1943.

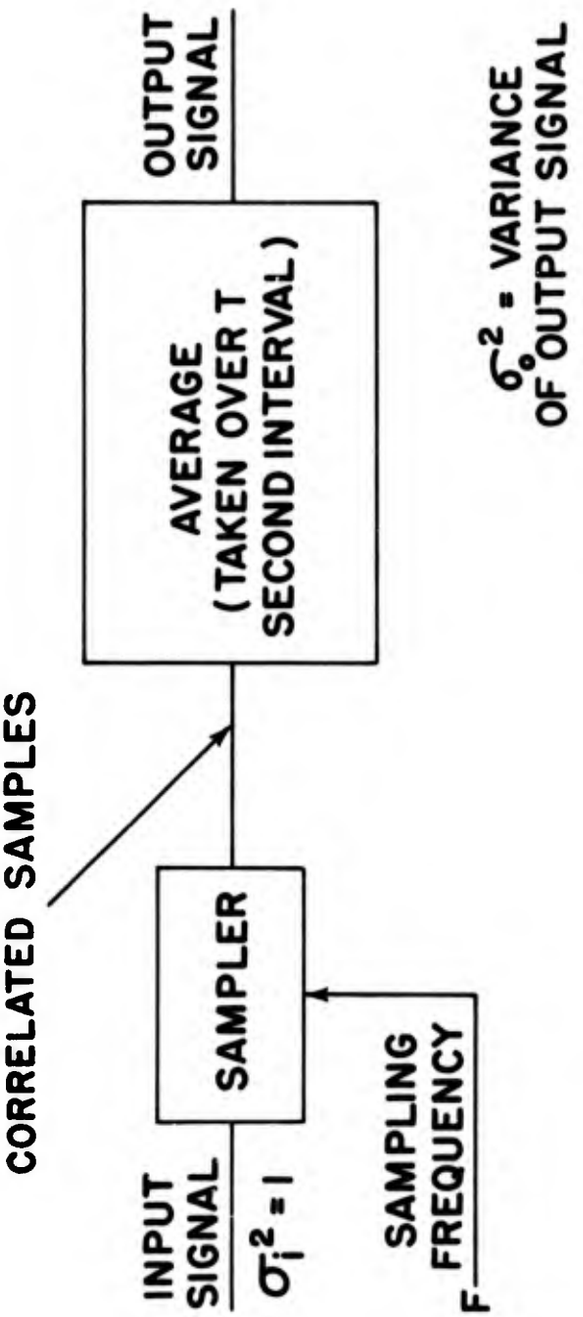

FIG. A-1 AVERAGING SYSTEM BEING USED FOR ANALYSIS

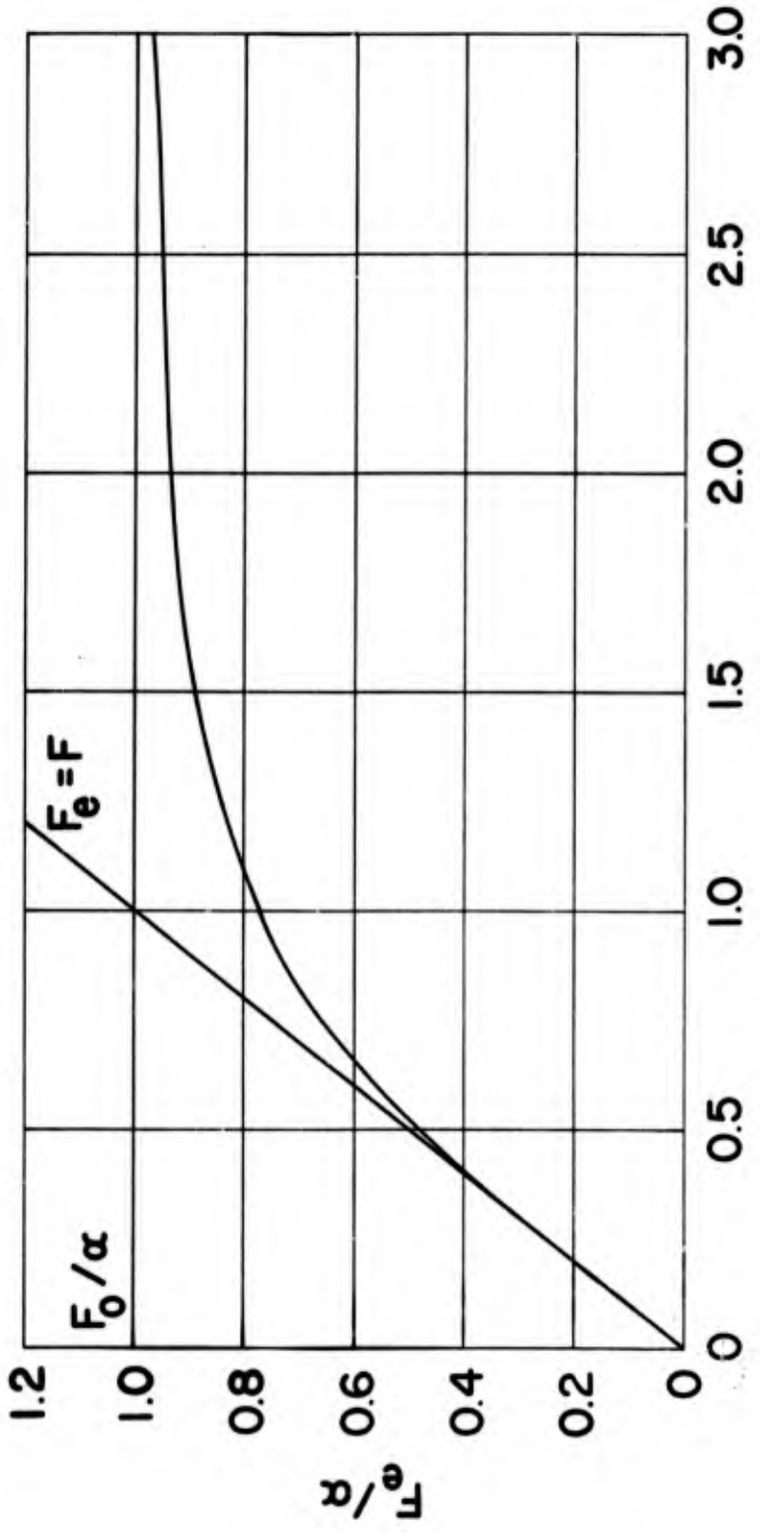

FIG. A-2 F_e vs F FOR RECTANGULAR SIGNAL WITH POISSON ZERO-CROSSINGS

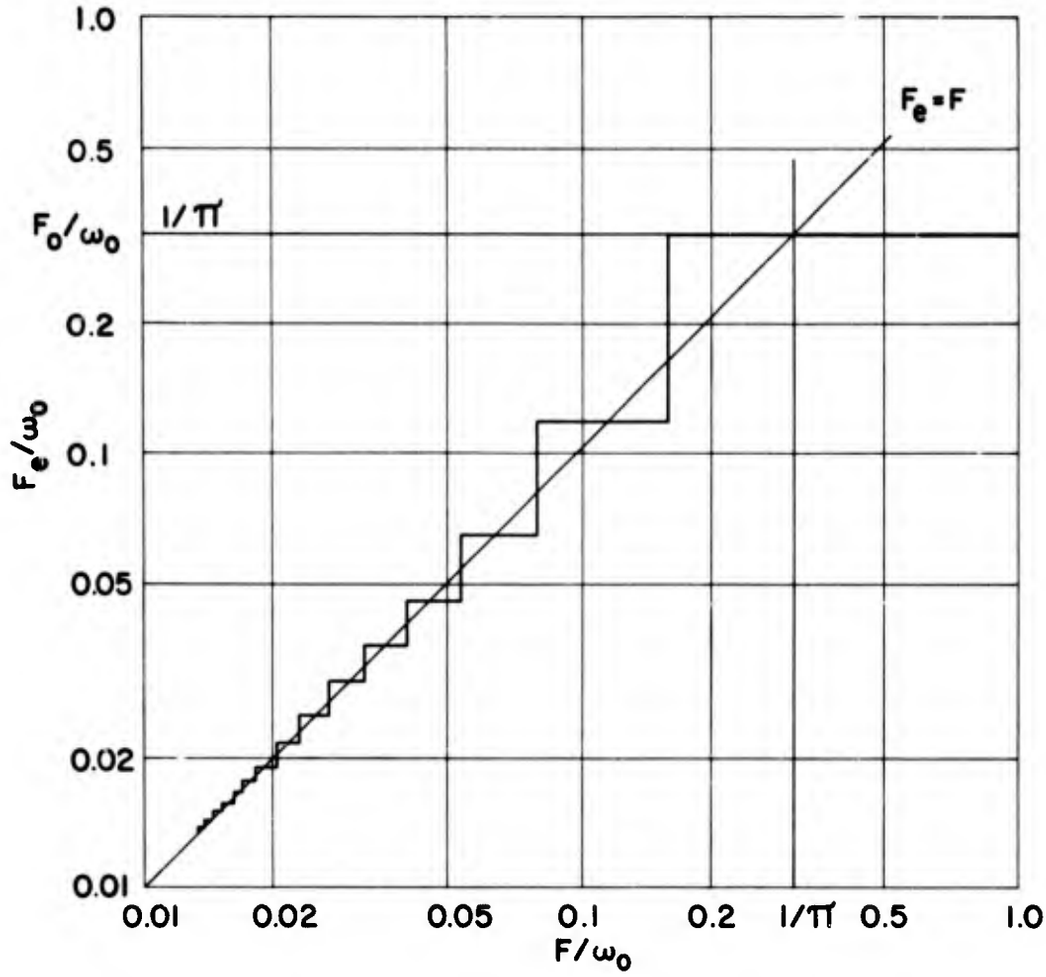

FIG. A-3 F_e vs F FOR IDEAL BAND-LIMITED SIGNAL

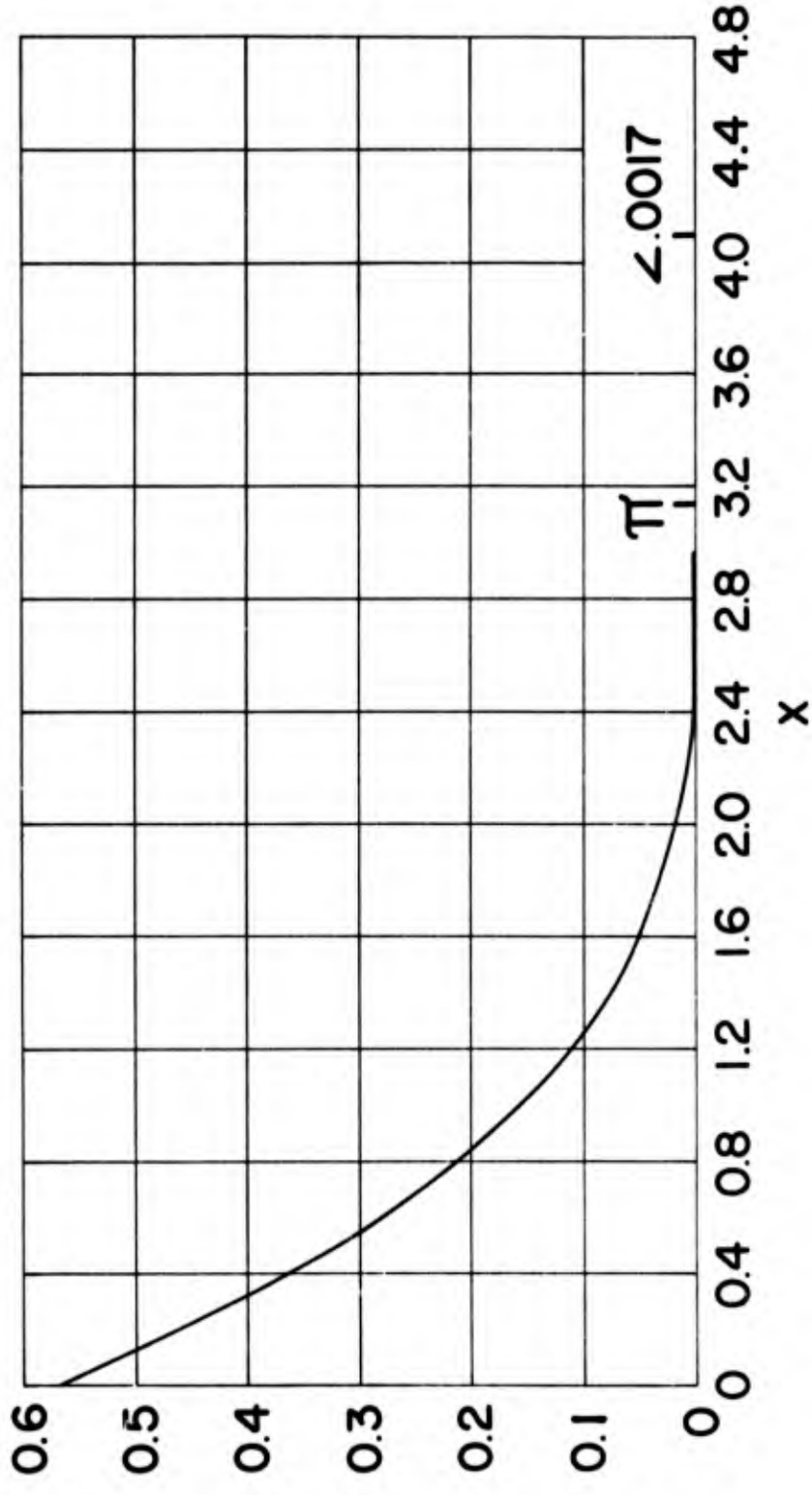

FIG. A-4 PLOT OF ARCSIN $(\frac{\sin X}{X}) - (\frac{\sin X}{X})$

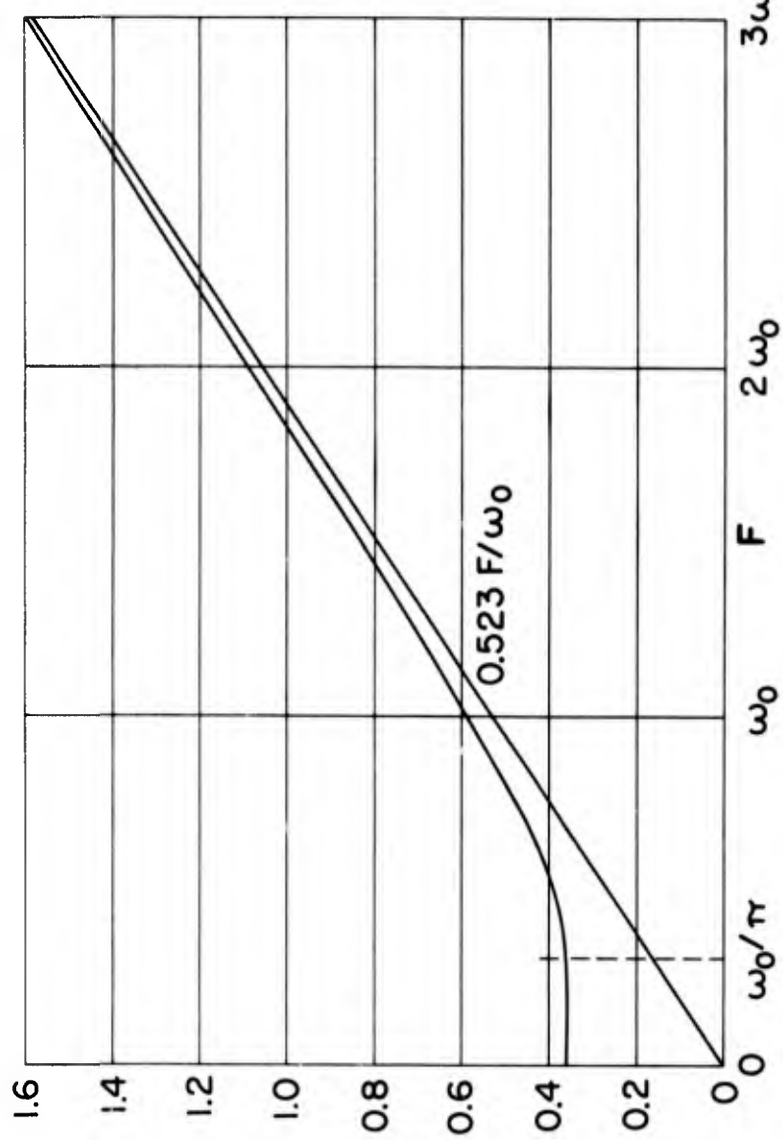

$$\text{PLOT OF } \sum_{K=-\infty}^{\infty} \theta_{bb}\left(\frac{K}{F}\right)=\frac{2}{\pi}\sum_{K=-\infty}^{\infty}\left[\text{ARCSIN}\left(\frac{\text{SIN}\,\frac{K\omega_0}{F}}{\frac{K\omega_0}{F}}\right)-\frac{\text{SIN}\,\frac{K\omega_0}{F}}{\frac{K\omega_0}{F}}\right]$$

FIG. A-5

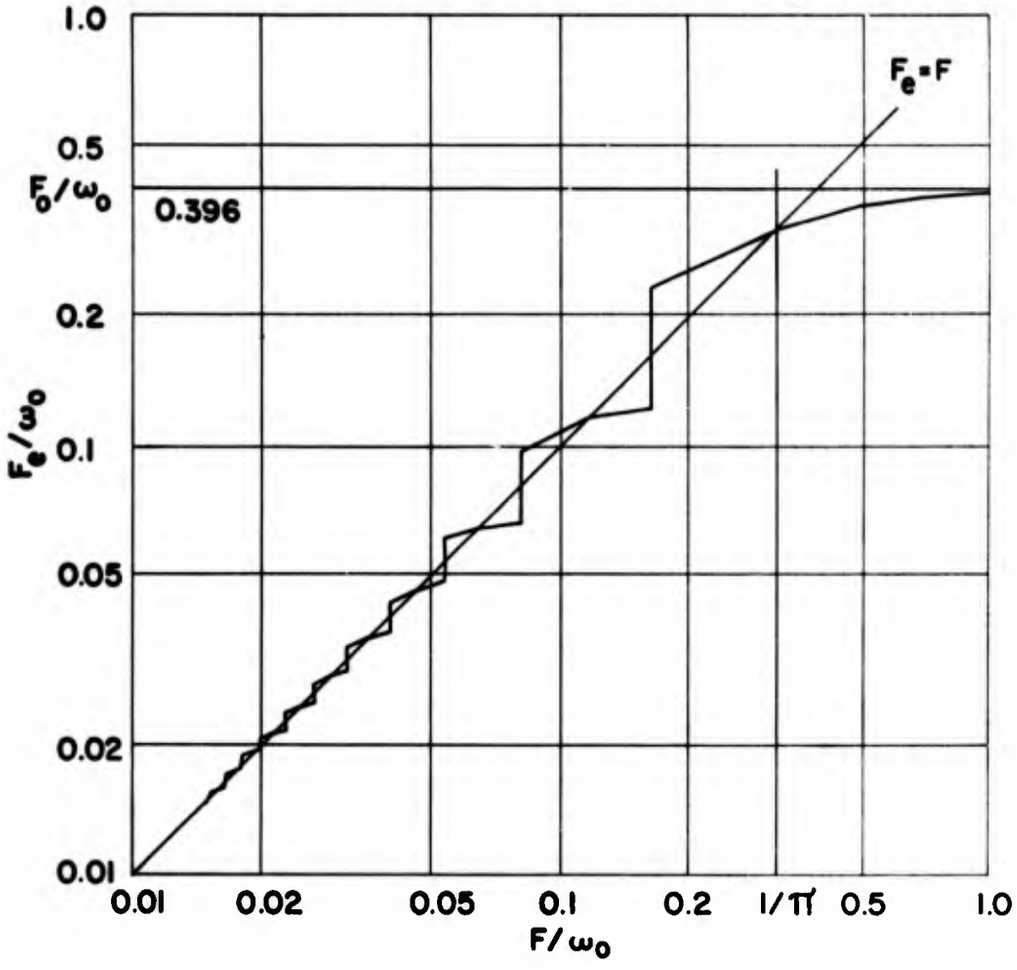

FIG. A-6 F_e vs F FOR CLIPPED BAND-LIMITED SIGNAL

BLANK PAGE

APPENDIX B

SPECTRUM OUT OF A SQUARE LAW DETECTOR WITH NARROW-BAND INPUT

A sinusoidal signal of frequency ω_o and power S may be written in the form $C_2 \cos\omega_o t$, where the time origin is chosen to make the phase zero and $C^2/2$ equals the power S. A narrow band random process at the frequency ω_o may be characterized by $\cos\omega_o t$ and $\sin\omega_o t$ terms, each multiplied by slowly varying time functions with zero mean gaussian distributions. Thus a sine wave in narrow band noise may be written in the form

$$f(t) = A(t) \sin\omega_o t + [B(t) + C] \cos\omega_o t \qquad \text{(B-1)}$$

The random functions A(t) and B(t) are independent gaussian variables which can be fully characterized by their autocorrelation function

$$\overline{A(t)\ A(t+\tau)} = \overline{B(t)\ B(t+\tau)} = \varphi_{SS}(\tau) \qquad \text{(B-2)}$$

Note the variance of either A or B equals $\varphi_{SS}(0)$ and is equal to the total noise power P in f(t). An alternative representation of A and B is by use of their power density spectrum, defined by the fourier transform pair

$$\Phi_{SS}(\omega) = \int_{-\infty}^{\infty} \varphi_{SS}(\tau) \exp(-j\omega\tau) d\tau \qquad \text{(B-3)}$$

$$\varphi_{SS}(\tau) = (1/2\pi) \int_{-\infty}^{\infty} \Phi_{SS}(\omega) \exp(j\omega\tau) d\omega \qquad \text{(B-4)}$$

Note that the double-sided low-pass spectrum $\phi_{SS}(\omega)$ is the same shape as the narrow-band power spectrum of f(t) centered around ω_o.

If f(t) is passed through a square-law detector, the function $x(t) = f^2(t)$ is produced. This function has terms centered around zero frequency and additional terms centered around $2\omega_o$. The narrow band approximation assumes that ω_o is appreciably greater than the bandwidth of the noise, so the double-frequency components can be eliminated easily by filtering. The remaining terms of x(t) are then

$$x(t) = (1/2)[A^2(t) + B^2(t) + 2C \cdot B(t) + C^2] \qquad \text{(B-5)}$$

The expected value or mean of x(t) can be found simply as

$$\begin{aligned} x(t) &= (1/2)[\overline{A^2} + \overline{B^2} + 2C\cdot\overline{B} + C^2] \\ &= (1/2)\ (P + P + 2C\cdot 0 + C^2) \\ &= P + C^2/2 = P + S \end{aligned} \tag{B-6}$$

so the mean output of the detector is simply the total signal plus noise power into the detector.

The variance of x(t) around this mean is obtained from

$$\begin{aligned} \sigma^2_x = \overline{x^2} - \overline{x}^2 &= (1/4)[\overline{A^4} + \overline{A^2B^2} + 2\overline{A^2BC} + \overline{A^2C^2} \\ &\quad + \overline{A^2B^2} + \overline{B^4} + 2\overline{B^3C} + \overline{B^2C^2} + 2\overline{A^2BC} + 2\overline{B^3C} \\ &\quad + 4\overline{B^2C^2} + 2\overline{BC^3} + \overline{A^2C^2} + \overline{B^2C^2} + 2\overline{BC^3} + C^4] \\ &\quad - (P^2 + 2PS + S^2) \\ &= (1/4)(3P^2 + P^2 + 0 + PC^2 + P^2 + 3P^2 + 0 \\ &\quad + PC^2 + 0 + 0 + 4PC^2 + 0 + PC^2 + PC^2 + 0 + C^4) \\ &\quad - (P^2 + 2PS + S^2) \end{aligned}$$

where use was taken of independence between A and B, the fact that all odd moments of A and B are zero, and the value $3P^2$ of the fourth moment of A and B. Simplifying further

$$\begin{aligned} \sigma^2_x &= (1/4)(8P^2 + 8PC^2 + C^4) - (P^2 + 2PS + S^2) \\ &= P^2 + 2PS \end{aligned} \tag{B-7}$$

This represents the noise in measurement of the output of the square law detector, for a single measurement.

If a number of measurements of the detector output are to be averaged for additional smoothing, it is necessary to know the spectral content or the autocorrelation of x(t). This is obtained by computing the autocorrelation function of x(t) from the form

$$\varphi_{xx}(\tau) = (1/4) \cdot \overline{[A^2(t)+B^2(t)+2C\cdot B(t)+C^2][A^2(t+\tau)+B^2(t+\tau)+2C\cdot B(t+\tau)+C^2]}$$

$$= (1/4)[\overline{A^2(t)A^2(t+\tau)} + \overline{A^2(t)B^2(t+\tau)} + 2C\cdot\overline{A^2(t)B(t+\tau)}$$

$$+ C^2\cdot\overline{A^2(t)} + \overline{B^2(t)A^2(t+\tau)} + \overline{B^2(t)B^2(t+\tau)} + 2C\cdot\overline{B^2(t)B(t+\tau)}$$

$$+ C^2\cdot\overline{B^2(t)} + 2C\cdot\overline{B(t)A^2(t+\tau)} + 2C\cdot\overline{B(t)B^2(t+\tau)}$$

$$+ 4C^2\cdot\overline{B(t)B(t+\tau)} + 2C^3\cdot\overline{B(t)} + C^2\cdot\overline{A^2(t+\tau)} + C^2\cdot\overline{B^2(t+\tau)}$$

$$+ 2C^3\overline{B(t+\tau)} + C^4]$$

$$= (1/4)\ [2\varphi_{SS}{}^2(\tau) + P^2 + P^2 + 0 + C^2P + P^2$$

$$+ 2\varphi_{SS}{}^2(\tau) + P^2 + 0 + C^2P + 0 + 0 + 4C^2\varphi_{SS}(\tau)$$

$$+ 0 + C^2P + C^2P + 0 + C^4]$$

$$= \varphi_{SS}{}^2(\tau) + C^2\varphi_{SS}(\tau) + P^2 + C^2P + C^2/4$$

$$= \varphi_{SS}{}^2(\tau) + 2S\varphi_{SS}(\tau) + (P + S)^2 \qquad \text{(B-8)}$$

where use has been made of the fact that for gaussian variables

$$\overline{WXYZ} = \overline{WX}\ \overline{YZ} + \overline{WY}\ \overline{XZ} + \overline{WZ}\ \overline{XY}$$

to evaluate the fourth moments.

Equation (B-8) may be interpreted most easily by writing the autocorrelation function in a normalized form

$$n\varphi_{SS}(\tau) = \varphi_{SS}(\tau)/\varphi_{SS}(0) = \varphi_{SS}(\tau)/P$$

to give

$$\varphi_{xx}(\tau) = P^2\,{}_n\varphi_{SS}{}^2(\tau) + 2PS\,{}_n\varphi_{SS}(\tau) + (P + S)^2 \qquad \text{(B-9)}$$

The first term of equation (B-9) is then a noise term of power P^2 whose spectrum is determined by the autocorrelation function ${}_n\varphi_{SS}{}^2(\tau)$, while the second term is a noise contribution of power 2PS whose spectrum is determined by ${}_n\varphi_{SS}(\tau)$. These correspond to the two terms of the variance given in equation (B-7) where the spectral information was not present. The third term of equation (B-9) is a constant and is simply the square of the mean value P+S obtained from the square law detector.

Notice that the second term has a power density spectrum ${}_n\Phi_{SS}(\omega)$ identical to the power density spectrum of the random functions A and B, but is present only when the signal power S is non-zero. The first term of equation (B-9) depends only on the noise power P, but has a different spectrum due to the squaring of the autocorrelation function. The spectral characteristics of this term may be determined directly in the frequency domain as

$$
\begin{aligned}
{}_n\Phi_{nn}(\omega) &= \int_{-\infty}^{\infty} {}_n\varphi_{SS}{}^2(\tau)\ \exp\ (-j\omega\tau)d\tau \\
&= (1/2\pi)\int_{-\infty}^{\infty} {}_n\varphi_{SS}(\tau)\int_{-\infty}^{\infty} {}_n\Phi_{SS}(\alpha)\ \exp(j\alpha\tau)\ \exp(-j\omega\tau)\ d\alpha d\tau \\
&= (1/2\pi)\int_{-\infty}^{\infty} {}_n\Phi_{SS}(\alpha)\int_{-\infty}^{\infty} {}_n\varphi_{SS}(\tau)\ \exp\ (-j(\omega-\alpha)\tau)\ d\tau d\alpha \\
&= (1/2\pi)\int_{-\infty}^{\infty} {}_n\Phi_{SS}(\alpha)\ \ {}_n\Phi_{SS}(\omega-\alpha)\ d\alpha \qquad \text{(B-10)}
\end{aligned}
$$

or an auto-convolution of the normalized input noise spectrum

$${}_n\Phi_{SS}(\omega) = \Phi_{SS}(\omega)/P.$$

Thus in summary, the output of the square law detector consists of a constant term of value P + S, a noise term of variance 2PS with a spectrum identical to the normalized low-pass spectrum ${}_n\Phi_{SS}(\omega)$ of the detector noise input, and a noise term of variance P^2 whose auto-correlation function is the square of that of the input noise envelope or whose normalized power density spectrum is given by equation (B-10).

Unclassified
Security Classification

DOCUMENT CONTROL DATA - R & D

(Security classification of title, body of abstract and indexing annotation must be entered when the overall report is classified)

1. ORIGINATING ACTIVITY *(Corporate author)*

Naval Ordnance Laboratory
Silver Spring, Maryland 20910

2a. REPORT SECURITY CLASSIFICATION

Unclassified

2b. GROUP

3. REPORT TITLE

Effect of Finite Sampling Rates on Smoothing the Output of a Square Law Detector with Narrow Band Input

4. DESCRIPTIVE NOTES *(Type of report and inclusive dates)*

5. AUTHOR(S) *(First name, middle initial, last name)*

Pryor, C. Nicholas

6. REPORT DATE	7a. TOTAL NO. OF PAGES	7b. NO. OF REFS
2/26/71	52	6

8a. CONTRACT OR GRANT NO	9a. ORIGINATOR'S REPORT NUMBER(S)
b. PROJECT NO. A370-370A-WF08-121-703	NOLTR 71-29
c.	9b. OTHER REPORT NO(S) *(Any other numbers that may be assigned this report)*
d.	

10. DISTRIBUTION STATEMENT

This document is subject to special export controls and each transmittal to foreign governments or foreign nationals may be made only with prior approval of NOL.

11. SUPPLEMENTARY NOTES	12. SPONSORING MILITARY ACTIVITY
	Naval Air Systems Command

13. ABSTRACT

Most modern spectral analysis systems time-share a single narrow-band filter and detector among a large number of frequency channels and thus provide sampled rather than continuous data to output averaging devices. For practical filter designs and finite sampling rates, a loss in performance is experienced due to this sampling. Analytical means are developed for computing this loss, and the loss is evaluated for a number of common filter shapes. Losses of 1 to 2 dB are shown to occur when the detector is sampled at rates comparable to the detector bandwidth.

DD FORM 1 NOV 65 1473 (PAGE 1)

S/N 0101-807-6801

Unclassified
Security Classification

14 KEY WORDS	LINK A		LINK B		LINK C	
	ROLE	WT	ROLE	WT	ROLE	WT
Signal Processing Spectral Analysis Fourier Transform Sampling Detection						